Some Common Ingredients for Heavy Orographic Rainfall

YUH-LANG LIN AND SEN CHIAO

Department of Marine, Earth and Atmospheric Sciences, North Carolina State University, Raleigh, North Carolina

TING-AN WANG

Science and Technology Advisory Group, The Executive Yuan, Taiwan

MICHAEL L. KAPLAN

Department of Marine, Earth and Atmospheric Sciences, North Carolina State University, Raleigh, North Carolina

RONALD P. WEGLARZ

Department of Physics, Astronomy, and Meteorology, Western Connecticut State University, Danbury, Connecticut

(Manuscript received 6 November 2000, in final form 30 June 2001)

ABSTRACT

The purpose of this paper is to synthesize some common synoptic and mesoscale environments conducive to heavy orographic rainfall. Previous studies of U.S. and Alpine cases and new analyses of some Alpine and east Asian cases have shown the following common synoptic and mesoscale environments are conducive to heavy orographic rainfall: 1) a conditionally or potentially unstable airstream impinging on the mountains, 2) a very moist low-level jet (LLJ), 3) a steep mountain, and 4) a quasi-stationary synoptic system to slow the convective system over the threat area. A deep short-wave trough is found to approach the threat area in the U.S. and European cases, but is not found in the east Asian cases. On the other hand, a high convective available potential energy (CAPE) value is observed in east Asian cases, but is not consistently observed in the U.S. and European cases. The enhancement of low-level upward motion and the increase of instability below the trough by the approaching deep short-wave trough in the U.S. and Alpine events may partially compensate the roles played by high CAPE in the East Asian events. In addition, the concave mountain geometry plays an important role in helping trigger the convection in Alpine and Taiwanese cases.

Based on an ingredient argument, it is found that a heavy orographic rainfall requires significant contributions from any combinations of the above four common synoptic and mesoscale environments or ingredients, and high precipitation efficiency of the incoming airstream, strong upward motion, and large convective system. These ingredients are also used to help explain the synoptic and mesoscale environments observed in some orographic flooding and heavy rainfall events in other regions, such as in New Zealand, China, and India. An index, $U(\partial h/\partial x)q$, where U is the flow velocity perpendicular to the mountain range, $\partial h/\partial x$ the mountain slope, and q the water vapor mixing ratio, is also proposed to help predict the occurrence of heavy orographic rainfall. Estimates of this proposed index indicate that it may serve as a good indicator for predicting east Asian heavy orographic rainfall events.

1. Introduction

One of the most challenging and difficult problems in numerical weather prediction is quantitative precipitation forecasting, especially the prediction of orographically induced heavy precipitation (Smith et al. 1997). A significant number of heavy orographic rainfall events have occurred over mesoscale mountain ranges. These mountain ranges have a width of several hundred kilometers, and include the U.S. Rockies and Appalachians, the European Alps, the Western Ghats in India, the Central Mountain Range in Taiwan, mountains on the islands of Japan, the Southern Island of New Zealand, and others. These heavy orographic rainfall events may induce flash flooding and produce significant loss of life and substantial disruption of the local economy. Thus, to help improve the prediction of the occurrence of heavy orographic rainfall, it is important to identify some common synoptic and mesoscale environments typically associated with these events.

Based on the formation mechanisms of orographic rain proposed in previous studies (e.g., Smith 1979;

Corresponding author address: Prof. Yuh-Lang Lin, Dept. of Marine, Earth and Atmospheric Sciences, Box 8208, North Carolina State University, Raleigh, NC 27695-8208.
E-mail: yl_lin@ncsu.edu

Houze 1993; Lin 1993; Chu and Lin 2000), the majority of heavy orographic rainfall events over mesoscale topography are caused by either 1) upslope rain in conjunction with conditional or potential instability, or 2) leeside convective rain either advected in from the upwind slope region (which is produced by sensible heating in the vicinity of the mountain peaks or triggered by convergence in situ). In order to trigger the instability, the orographic lifting should be strong enough to force air parcels to ascend to their level of free convection. Thus, the occurrence of orographic rainfall may be determined by the wind velocity perpendicular to the mountain range (U), the moist static stability (N_w) of the incoming airstream, and the mountain height (h_m). In fact, these three factors can be consolidated into a single nondimensional parameter, that is, the moist Froude number ($F_w = U/N_w h_m$), which may be used to predict the location and propagation of the orographically-induced convective systems.

Based on F_w, Chu and Lin (2000) identified three moist flow regimes for conditionally unstable flow over a two-dimensional mesoscale mountain: 1) upstream propagating convective systems, 2) quasi-stationary convective systems, and 3) quasi-stationary and downstream propagating convective systems. These three regimes correspond to small, moderate, and large values of F_w, respectively. Chu and Lin (2000) also found that heavy upslope rain might occur in the first two regimes. Recently, Chen and Lin (2001) have extended the work of Chu and Lin (2000) to include a three-dimensional mountain and found that heavy upslope rainfall may be produced in the presence of a low-level jet (LLJ). This is consistent with what is often observed in heavy orographic rainfall events, which occur in the United States (e.g., Maddox et al. 1978; Pontrelli et al. 1999), the European Alps (e.g., Buzzi et al. 1998) and in Taiwan (e.g., Chen and Yu 1988). However, in addition to the presence of an LLJ, it appears that some other synoptic and mesoscale features may also play important roles in controlling the generation of heavy orographic rain.

By examining heavy orographic rainfall events in the United States, such as the 1972 Black Hills flood in South Dakota, the 1977 Big Thompson Canyon flood in Colorado, the 1995 Madison County flood in Virginia, and the 1997 Fort Collins flood in Colorado, several authors (e.g., Maddox et al. 1978; Caracena et al. 1979; Caracena and Fritsch 1983; Pontrelli et al. 1999; Petersen et al. 1999) have found some common synoptic and mesoscale environmental features conducive to heavy orographic rainfall. We will briefly review these features in section 2, and then use them to examine and determine whether or not they exist in the heavy orographic rainfall events that have been observed in other regions, such as the European Alps, Taiwan, and Japan.

In the last decade, several flash flood events, which resulted from heavy orographic rainfall, have occurred on the southern slopes of the European Alps, such as the Vaison-la-Romaine flood of 22 September 1992 in France, the Brig flood of 24 September 1993 in Switzerland, the Piedmont flood of 4–6 November 1994 in Italy, and the South Ticino flood of 13–14 September 1995 in Switzerland. Many of these floods resulted in significant loss of life and substantial disruption of the local economy. In order to improve quantitative precipitation forecasts associated with this type of heavy orographic rain, a field experiment (the Mesoscale Alpine Program, MAP) held in fall 1999 was proposed by the international meteorological community to investigate the problem (Binder and Schär 1996; Bougeault et al. 2001). In this study, we will examine the common synoptic and mesoscale environments conducive to heavy orographic rainfall events observed in the United States and compare them to some Alpine events.

On 6 August 1999, Tropical Storm Rachel moved slowly toward Taiwan, and was then strongly influenced by the Central Mountain Range (CMR), while Typhoon Paul was located to the northeast and a cold-core low centered in the upper troposphere was located over the east coast of China. During the night of 7 August 1999, southwestern Taiwan experienced heavy rainfall and flash flooding. The local maximum rainfall totaled 347 mm by the end of the event. In fact, the rain started even before the tropical storm was close to Taiwan, which raises an important question. What are the common synoptic and mesoscale environmental features conducive to heavy orographic rainfall for this particular event, as compared to other events over Taiwan's CMR?

In order to identify these features, we will examine a flash flood event, which occurred in Taiwan on 7 August 1959. The 1959 flash flood in Taiwan produced a maximum rainfall rate of more than 1000 mm within a 16-h time period. Interestingly, the synoptic and mesoscale environmental features associated with the 1959 case were very similar to those accompanying the 1999 case. Both cases were associated with a tropical storm or depression moving toward Taiwan's CMR while a preexisting typhoon was located northeast of Taiwan. In addition to these two events that occurred in Taiwan, we will also investigate a heavy orographic rainfall event that occurred in Japan, and that was also caused by an approaching tropical depression.

The purpose of this study is to synthesize the common synoptic and mesoscale environments conducive to heavy orographic rainfall events in the United States, the European Alps, and east Asia. This paper is organized as follows. In section 2, we will give a review and discuss the synoptic and mesoscale environment features conducive to heavy orographic rainfall events, which have occurred in the vicinity of U.S. mountain ranges. In section 3, we will examine conditions for some heavy rainfall events over the European Alps and which occurred during the second MAP Intensive Observation Period (IOP2). In section 4, we will examine two events, one of which occurred in Taiwan, the other in Japan that resulted from interactions between tropical storms and/or depressions and the island topography. In

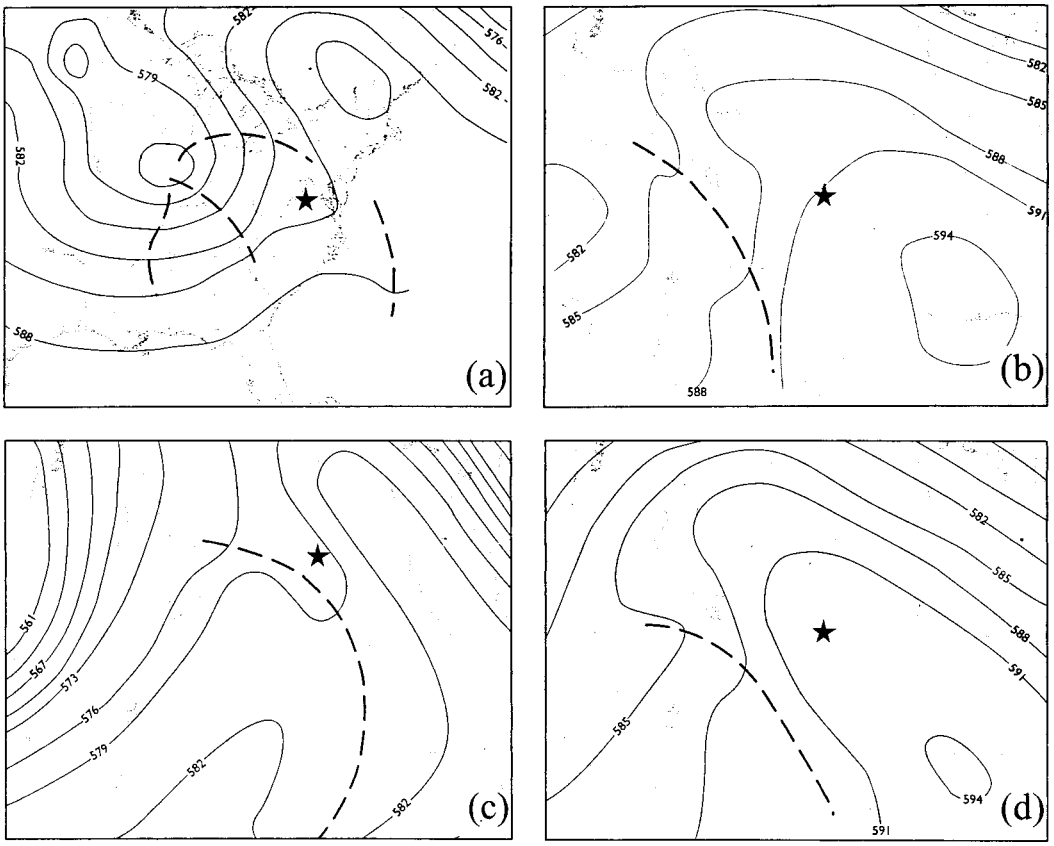

FIG. 1. The 500-hPa height analyses near the onset time of severe flash floods: (a) Madison County, VA (1200 UTC 27 Jun 1995); (b) Fort Collins, CO (0000 UTC 29 Jul 1997); (c) Rapid City, SD (0000 UTC 10 Jun 1972); and (d) Big Thompson Canyon, CO (0000 UTC 1 Aug 1976). Shown are storm locations (star), heights (solid lines, 3-dam intervals), and short-wave trough axes (bold dashed lines). [After Pontrelli et al. (1999).]

section 5, we will propose several common ingredients for producing heavy orographic rainfall. A summary is given in section 6.

2. A review of synoptic and mesoscale environments conducive to heavy orographic rainfall in the United States

By comparing the 1972 Black Hills flood in South Dakota and the 1977 Big Thompson Canyon flood in Colorado, Maddox et al. (1978) found the following common *synoptic features*: 1) A middle- and upper-tropospheric trough lies over the western United States with a negatively tilted ridge just east of the threat area (Figs. 1c and 1d). 2) A weak 500-hPa short-wave trough rotates northward in the long-wave trough and approaches the threat area (Figs. 1c and 1d). 3) Light (5–20 kt) southeast to south-southeastly winds are present in the upper troposphere over the threat area (Figs. 2c and 2d). 4) A slow moving or stationary polar front lies just south of the threat area (Figs. 2c and 2d). 5) High moisture content is present through a deep layer (from the surface up through 300 hPa) (Figs. 3c and 3d). In addition, they also found the following *mesoscale features* shared by these two flash flood events: 1) Afternoon heating west of the threat area and cold advection east of storm area combine to intensify thickness and pressure gradients. The low-level wind flow maximizes near sunset. 2) A narrow band of conditionally unstable (lifted index $= -4$ to -7) and unusually moist (water vapor mixing ratio of 13–15 g kg^{-1}) air moves southward and westward behind the polar front (Figs. 2c and 2d). This air mass is capped by a temperature inversion near 700 mb (Figs. 3c and 3d). 3) Orographic lifting provides the mechanism needed to release the conditional instability, which produces heavy rainfall over middle elevations of the affected drainage. 4) Convective cells move slowly north-northwestward and continued cell redevelopment on the southeast flank of the thunderstorm complex results in a quasi-stationary precipitation system. Note that flash floods in the western United States are very complicated and have been categorized into four types by Maddox et al. (1980).

During the evening of 28 July 1997, the city of Fort Collins, Colorado, experienced a devastating flash flood that caused five fatalities and over $200 million in damage. Maximum accumulated rainfall exceeded 254 mm within 6 h. Prominent synoptic and mesoscale features

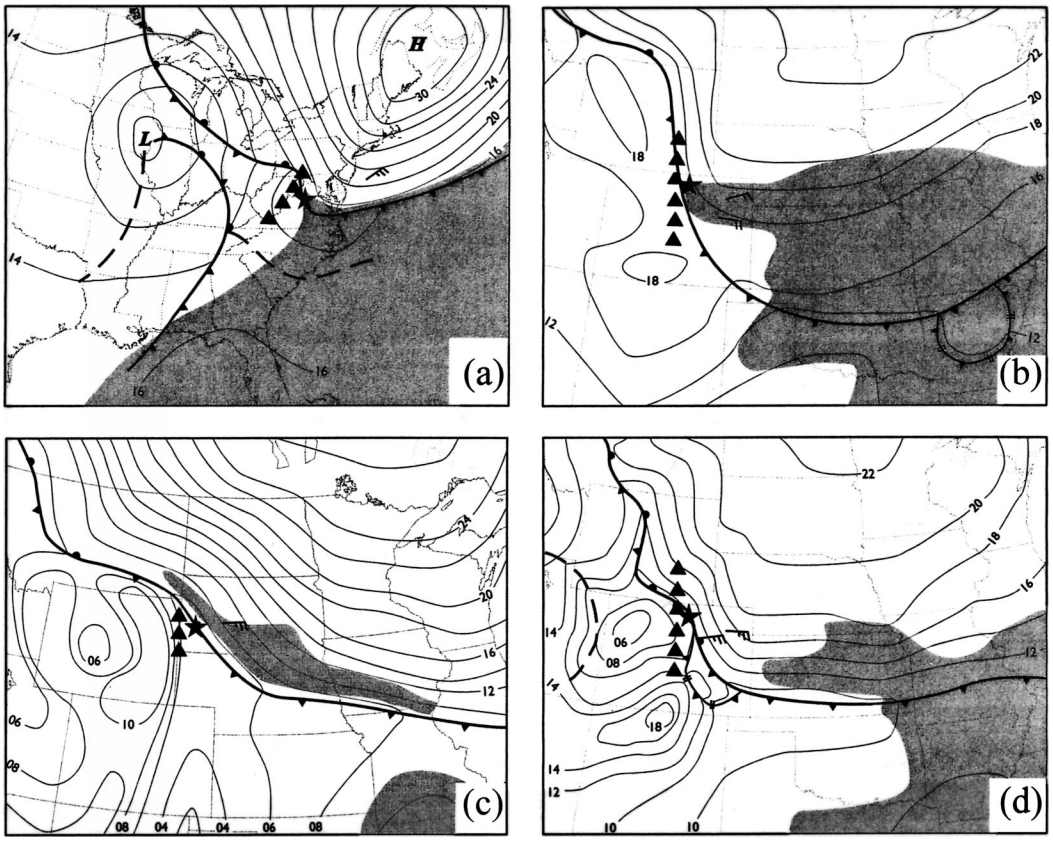

FIG. 2. Same as in Fig. 1 [(a) Madison County flood, (b) Fort Collins flood, (c) Rapid City flood, (d) Big Thompson flood] except for surface winds near the storm (full barb = 5 m s^{-1}) and very moist region [shaded with dewpoint >(a) 22°C, (b) 17.7°C, (c) and (d) 18.3°C]. The mountains near the threat areas are denoted roughly by triangles. [Adapted from Pontrelli et al. (1999).]

(Petersen et al. 1999) included 1) the presence of a 500-hPa ridge axis over northeastern Colorado (Fig. 1b); 2) a weak short-wave trough on the western side of the high pressure ridge (Fig. 1b); 3) a strong, moist post-frontal easterly upslope flow at low levels (Fig. 2b); 4) weak to moderate southwesterly flow aloft (Fig. 3b); 5) a deep, moist warm layer in the sounding (Fig. 3b); 6) the presence of a quasi-stationary convective system; and 7) low convective available potential energy (CAPE). In contrast to the Rapid City and Big Thompson Canyon floods, the environmental atmosphere of the Fort Collins storm was only modestly conditionally unstable, based on the observed values of CAPE (not shown). Note that CAPE is of mesoscale nature, it can vary greatly from time to time and from place to place. In addition, an accelerated easterly and low-level wind during the last 1.5 h of the event impinged on the mountains and induced a quasi-stationary convective system causing the heaviest rainfall to be located directly over Fort Collins. Therefore, the synoptic conditions found in the orographic flash flood events of Rapid City and Big Thompson Canyon (Maddox et al. 1978) also apply to the Fort Collins flood. Mesoscale conditions 2 and 4 proposed by Maddox et al. (1978) also appear to apply to the Fort Collins flood.

On 27 June 1995, after a convective system developed in the early morning, a second system formed over northeastern Madison County, Virginia; intensified; and propagated southeastward along the eastern slopes of the Blue Ridge Mountains. This system remained quasi-stationary over the western portions of the county, feeding off moist, conditionally unstable air flowing westward from the Atlantic Ocean (Pontrelli et al. 1999). Heavy downpours inundated the watershed of the Rapidan River throughout the morning and early afternoon causing record rainfall. Most of the rainfall that fell across the region resulted in the flash flooding, and reached a total amount of 344 mm (13.54 in.). Some observers recorded total precipitation in excess of 500 mm (19.68 in.), with about half of the precipitation falling within 2 h, and with maximum rainfall occurring on the upslope face of the Blue Ridge Mountains. Pontrelli et al. (1999) found that the synoptic conditions responsible for initiating and maintaining the Madison County storm were very similar to the Big Thompson Canyon and Fort Collins floods along the Front Range

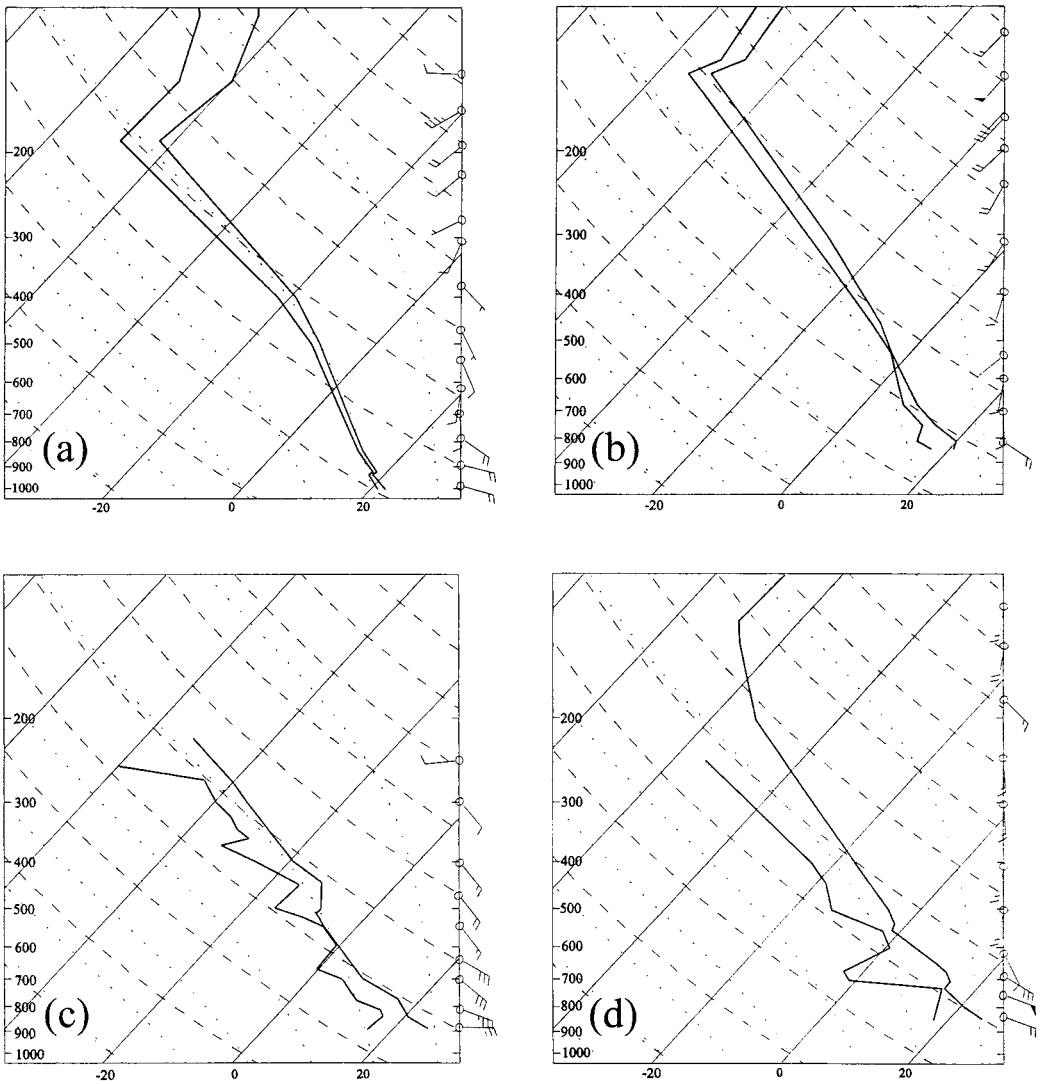

FIG. 3. Same as in Fig. 1 [(a) Madison County flood, (b) Fort Collins flood, (c) Rapid City flood, (d) Big Thompson flood] except for soundings near the onset time of severe leeside floods. [After Pontrelli et al. (1999).]

of the Rocky Mountains, as well as the Rapid City flood along the eastern slopes of the Black Hills of South Dakota. Because of Pontrelli et al.'s (1999) study (e.g., see Figs. 1a, 2a, and 3a) and studies by Maddox et al. (1978) and Petersen et al. (1999), the common synoptic and mesoscale features for these four events may be summarized as follows: 1) There exists a very strong upslope, LLJ from the east or southeast existed a southward propagating shallow cold front. 2) The LLJ has a very high equivalent potential temperature. 3) There exists an upper-tropospheric short-wave trough just upstream from the flood location, which is propagating toward the high pressure ridge axis. 4) There exists a massive middle- to upper-tropospheric westward-tilted ridge of high pressure. 5) Orographic lifting provides the necessary forcing needed to release the conditional instability. 6) Weak mid- and upper-tropospheric steering currents favored the slow moving storms that further contributed to locally excessive rainfall. These features are shown in Fig. 4. Note that a high value of CAPE is not consistently observed for these events.

3. Synoptic and mesoscale environments conducive to heavy orographic rainfall in the European Alps

The European Alps have a length of about 1000 km, a width of about 200 km, and are characterized by numerous peaks and valleys (Fig. 5). The highest peak reaches a height of about 4.8 km. In analyzing some heavy orographic precipitation events that have occurred over the southern Alps (e.g., the Vaison-la-Romaine event in France, the Brig and South Ticino events in Switzerland, and the Piedmont event in Italy) during

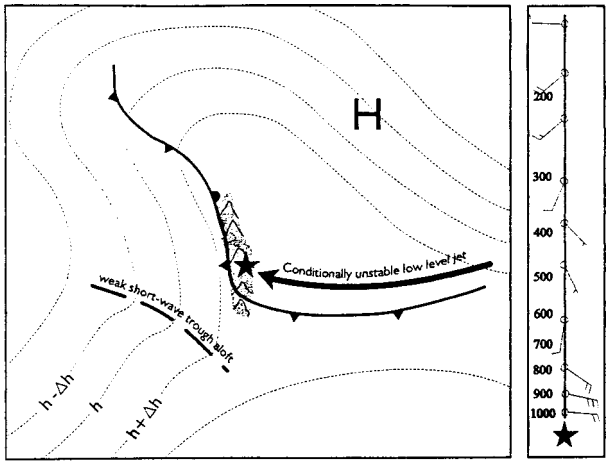

FIG. 4. Idealized schematic of the synoptic and mesoscale conditions conducive to heavy orographic rainfall. Shown are the threat region (star), 500-hPa height pattern (dotted lines), mountains (shaded), and typical wind profile above the threat region. [After Pontrelli et al. (1999).]

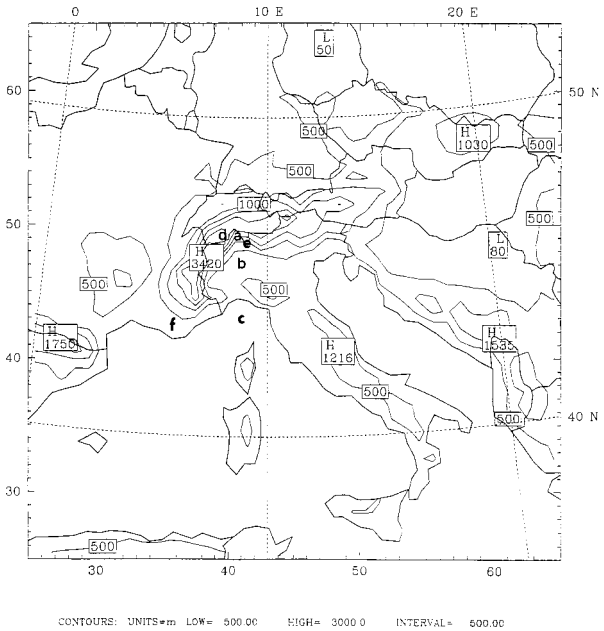

FIG. 5. Alps topography and geographic map of western Europe and Ligurian Sea. Orographic contour increment is 500 m. The numbers denote (a) Lago Maggiore area (Italy), (b) Piedmont area, (c) Ligurian Sea, (d) Brig (Switzerland), (e) South Ticino (Switzerland), and (f) Vaison-la-Romaine (France).

the fall season, Massacand et al. (1998) found that all these events were accompanied by a deep (~4 km), narrow (~500 km), and elongated (~2000 km) upper-tropospheric filament of extruded stratospheric air, which extended in a meridionally-oriented (north–south) direction from the British Isles to the western Mediterranean (see Fig. 6). In each case, the filament of stratospheric air translated relatively slowly eastward, and the storm event ensued as the filament's forward flank approached the Alpine ridge. Massacand et al. (1998) then proposed that these filaments constitute a streamer of high potential vorticity (PV) and act as a precursor for storms along the southern slopes of the European Alps. They proposed that these high PV streamers tend to 1) enhance the southerly flow component toward the Alps (i.e., form a low-level jet perpendicular to the mountain range), 2) reduce the static stability beneath the upper-level PV anomaly, and 3) trigger ascent on the PV streamer's forward flank to generate or enhance convection. The ascent induced by the forward (eastern) flank of the upper-level trough or PV streamer may coincide with the low-level orographically induced upward motion to trigger vigorous convection. Fehlmann and Quadri (2000) have used the southern part of the high PV anomalies that approach the European continent as a precursor to predict the precipitation on the southern side of the European Alps. They found that the predicted precipitation patterns for heavy orographic rainfall events on the southern slopes of the Alps could depend on the substructure of the PV filament.

In investigating heavy orographic rain over the southern Alps, Buzzi et al. (1995, 1998) and Buzzi and Foschini (2000) found that the following large and mesoscale flow features are important for allowing the persistence of strong upward motion and moisture convergence: 1) The flow at low levels maintains a southerly direction over the western Mediterranean, with pronounced confluence over the western Alps, between the postfrontal southwesterly flow and the prefrontal southeasterly flow located more to the east. 2) There exists an 850-hPa prefrontal LLJ that serves as a ''warm conveyor belt,'' which flows directly toward the Ligurian Apennines and the western Alps. 3) There exists a deep upper-tropospheric trough approaching the Alps. 4) There exists a quasi-stationary pressure ridge in the upper troposphere, located to the east, associated with an anticyclone over Eastern Europe. Buzzi et al. (1995) hypothesized that the scale contraction and intensification of the geopotential height gradient may occur on the eastern side of the trough.

It appears that the high PV streamers found by Massacand et al. (1998) are related to the deep short-wave trough found in Buzzi et al.'s studies. In addition, if one inspects Massacand et al.'s figures closely, it can be seen that there also exists a quasi-stationary pressure ridge to the east of the high PV streamer in all cases (Fig. 6), which was not emphasized in their paper. The low-level jets that occurred just before the onset of the heavy orographic rainfall events were partially associated with the approaching deep short-wave trough (Fig. 6). In other words, the approaching deep short-wave trough not only provides the upper-level divergence for additional upward motion over the upsloping topography on its forward (eastern) flank, but it also strengthens the LLJ and helps bring the deep layer of conditionally

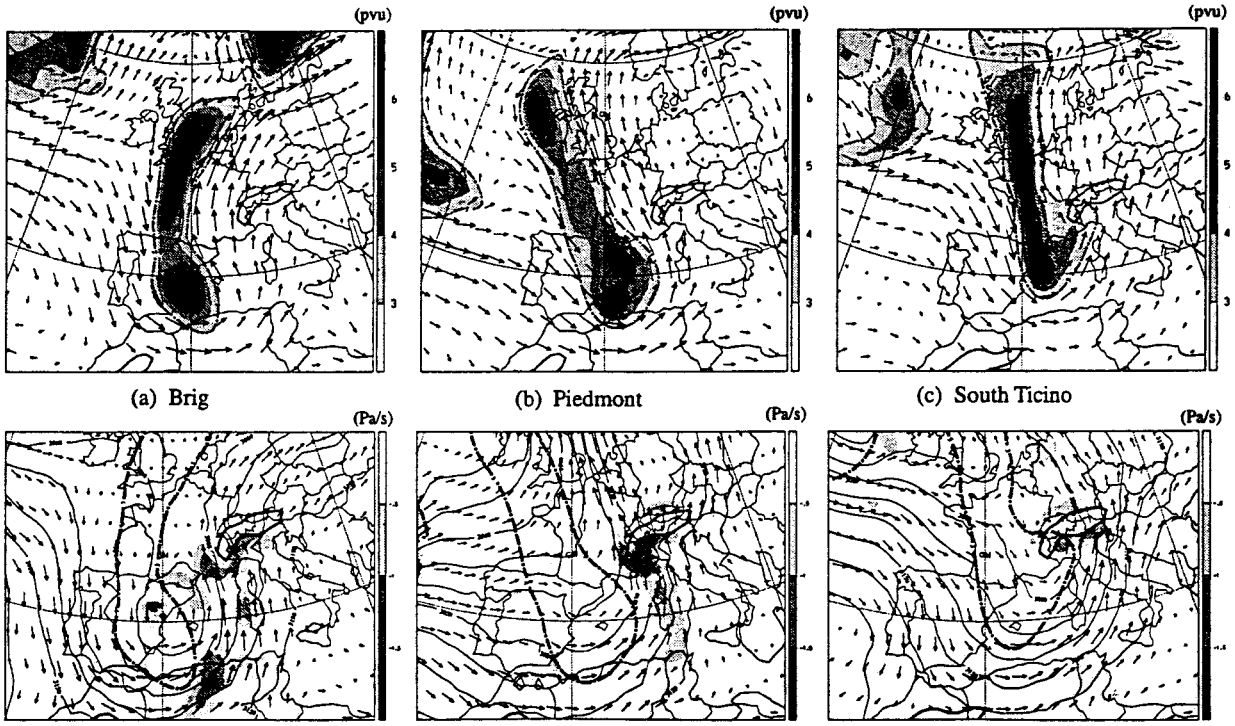

FIG. 6. Distribution of mean PV [shaded in PV units (pvu)] superimposed on 200-hPa wind vector field, and 3-pvu PV isolines and ascent (shaded in Pa s^{-1} superimposed upon 700-hPa wind vector field in upper and lower panels, respectively, for (a) Brig, 1200 UTC 23 Sep 1993; (b) Piedmont, 1800 UTC 5 Nov 1994; and (c) South Ticino, 1200 UTC 13 Sep 1995. Alpine region is outlined by thick solid line. [After Massacand et al. (1998).]

unstable air (e.g., see Fig. 7) from the Mediterranean Sea to interact with the Alpine mountains to produce diffluence and outflow aloft. Similar to U.S. events, high values of CAPE are not consistently observed in Alpine heavy orographic rainfall events. For example, the 1992 Vaison-la-Romaine case has a CAPE of 2662 J kg^{-1} (Table 1) at an upstream location, while the Piedmont (PDM) case only has a CAPE of 212 J kg^{-1} at 0000 UTC 5 November at PDM (Fig. 7). One particular flow feature associated with the majority of Alpine heavy orographic rainfall events is that convection often starts in the concave region south of the Alps, such as the Lago

TABLE 1. An estimate of the contributions from some common ingredients.

Event	NLLJ (U in m s)	Mountain slope ($\delta h/\delta x$)	q (g kg^{-1})	Index [U ($\delta h/\delta x$)q]	w_{env} (synoptic system)	Max rainfall rate	CAPE (J kg^{-1}) (selected)
Taiwan 1999	10.0	0.033	21	6.9	No	200 mm day^{-1}	2099
Taiwan 1959	17.5	0.033	22	12.7	No	500 mm day^{-1}	2406
Japan	17.5	0.020	19	6.7	No	150 mm day^{-1}	1149
Big Thompson, CO	12.5	0.025	16	5.0+*	Trough	915 mm day^{-1} [305 mm (4 h)$^{-1}$]	2526
Rapid City, SD	12.5	0.020	13.5	3.4+	Trough	1143 mm day^{-1} [381 mm (4 h)$^{-1}$]	— (<2180)
Fort Collins, CO	10	0.021	13	2.7+	Trough	519 mm day^{-1} [259 mm (6 h)$^{-1}$]	628
Madison County, VA	12.5	0.025	16	5.0+	Trough	600 mm day^{-1}	286
Vaison-la-Romaine, France	15	0.027	15	6.1+	Trough	300 mm day^{-1}	2662
Piedmont, Italy	13	0.033	11	4.7+	Trough	250 mm day^{-1}	212
South Ticino, Switzerland	10	0.033	9.3	3.1+	Trough	260 mm day^{-1} [130 mm (6 h)$^{-1}$]	383
Lago Maggiore, Italy (IOP2)	12.5	0.033	11.5	4.74+	Trough	300 mm (36 h)$^{-1}$	90

* Plus signs indicate that the index may be higher with the addition of w_{env} associated with an approaching synoptic system.

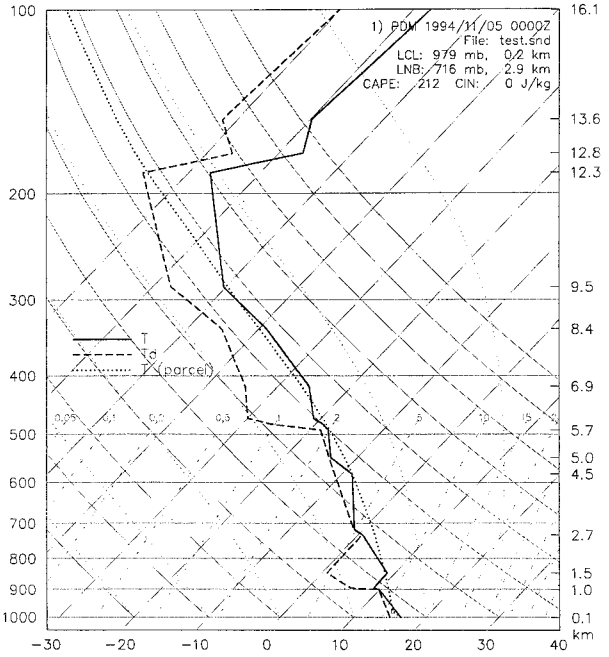

FIG. 7. Vertical temperature and dewpoint profiles of the radiosonde released from Palma de Mallorea (Piedmont flood) at 0000 UTC 5 Nov 1994.

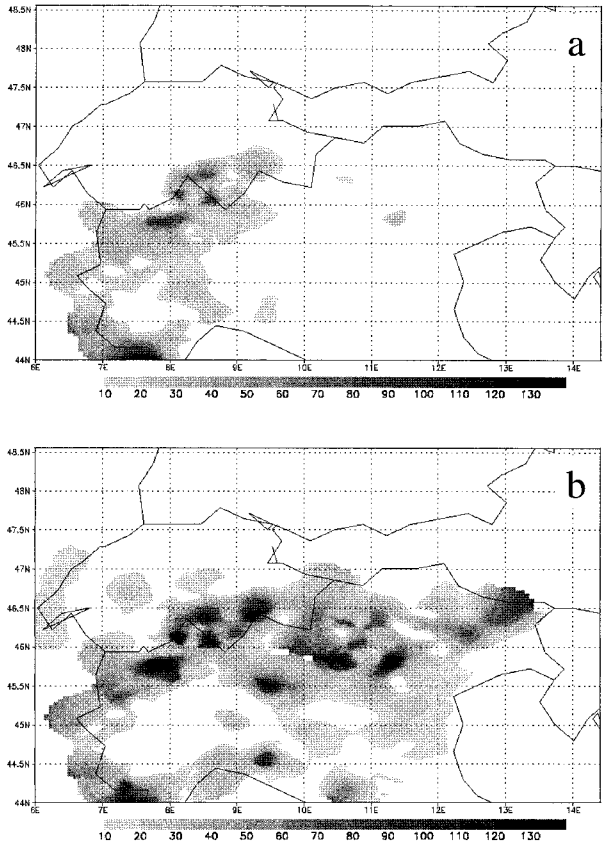

FIG. 8. Observed 12-h rainfall accumulations ending at (a) 0000 and (b) 1200 UTC 20 Sep 1999 for the MAP IOP2 heavy rainfall event.

Maggiore in Italy, and the Ticino region in Switzerland (Binder and Schär 1996; Buzzi and Foschini 2000). This confluent flow tends to enhance the low-level upward motion induced by the upslope, which in turn triggers the convection.

Figure 8 shows the accumulated 12-h rainfall ending at 0000 and 1200 UTC 20 September 1999 during the MAP IOP2 heavy orographic rainfall event. The rainfall accumulated during the whole event (1300 UTC 19 Sep–0100 UTC 21 Sep 1999) in the Lago Maggiore region in Italy ranges from 100 to 300 mm (Houze and Medina 2000). The rainfall region during the 12-h period ending at 0000 UTC 20 September (Fig. 8a) extended form the Gulf of Genoa to the Lago Maggiore region, with the heaviest precipitation focused in the Lago Maggiore area. The maximum 12-h rainfall amount reaches 130 mm. This heavy rainfall area apparently was associated with the impinging trough (Figs. 9a and 9c), which brought in from the Ligurian Sea air of high moisture content. Similar to the previously discussed historical events, the upper-level pressure ridge located to the east of the approaching deep short-wave trough is quasi-stationary (Figs. 9b and 9d). It can be seen clearly from Fig. 8 that the rainfall started in the Lago Maggiore region (Fig. 8a), which is located in the concave topography region of the southern slopes of the European Alps (see Fig. 5 for the mountain geometry). During the next 12-h period, ending 1200 UTC 20 September, the heavy rainfall encompassed the entire southern slopes of the Alps, where the maximum rainfall amount reached a value higher than 130 mm (Fig. 8b).

Figure 9 shows the surface and 300-hPa wind fields at 0000 and 1200 UTC 20 September 1999 associated with MAP IOP2. The impinging deep short-wave trough helped induce the southerly low-level jet, which reached a maximum value of about 12.5 m s^{-1} at Milan, Italy (Fig. 10a). CAPE values calculated from the Milan soundings were very small (149 and 201 J kg^{-1} at 0000 and 1200 UTC 20 Sep, respectively). Since CAPE may vary significantly with time and location, the estimates of CAPE from single soundings may not be representative of real CAPE values in the threat area. For example, the CAPE at Ajaccio, Corsica, at these two times were 0 and 22 J kg^{-1}, respectively (not shown). As also found in previous studies of historical flash flooding events over the southern Alps, the low-level jet is very moist, as revealed by the sounding data at Milan (Fig. 10). This low-level jet has a tongue of high moisture with water vapor mixing ratio (q_v) greater than 11 g kg^{-1} covering northern Italy and the Lago Maggiore region (Fig. 11a). The water vapor mixing ratio was increasing during the heavy rainfall period for the next 12 h (Fig. 11b).

In summary, similar to the U.S. cases, the synoptic and mesoscale environments conducive to heavy orographic rainfall in the European Alps are 1) a condi-

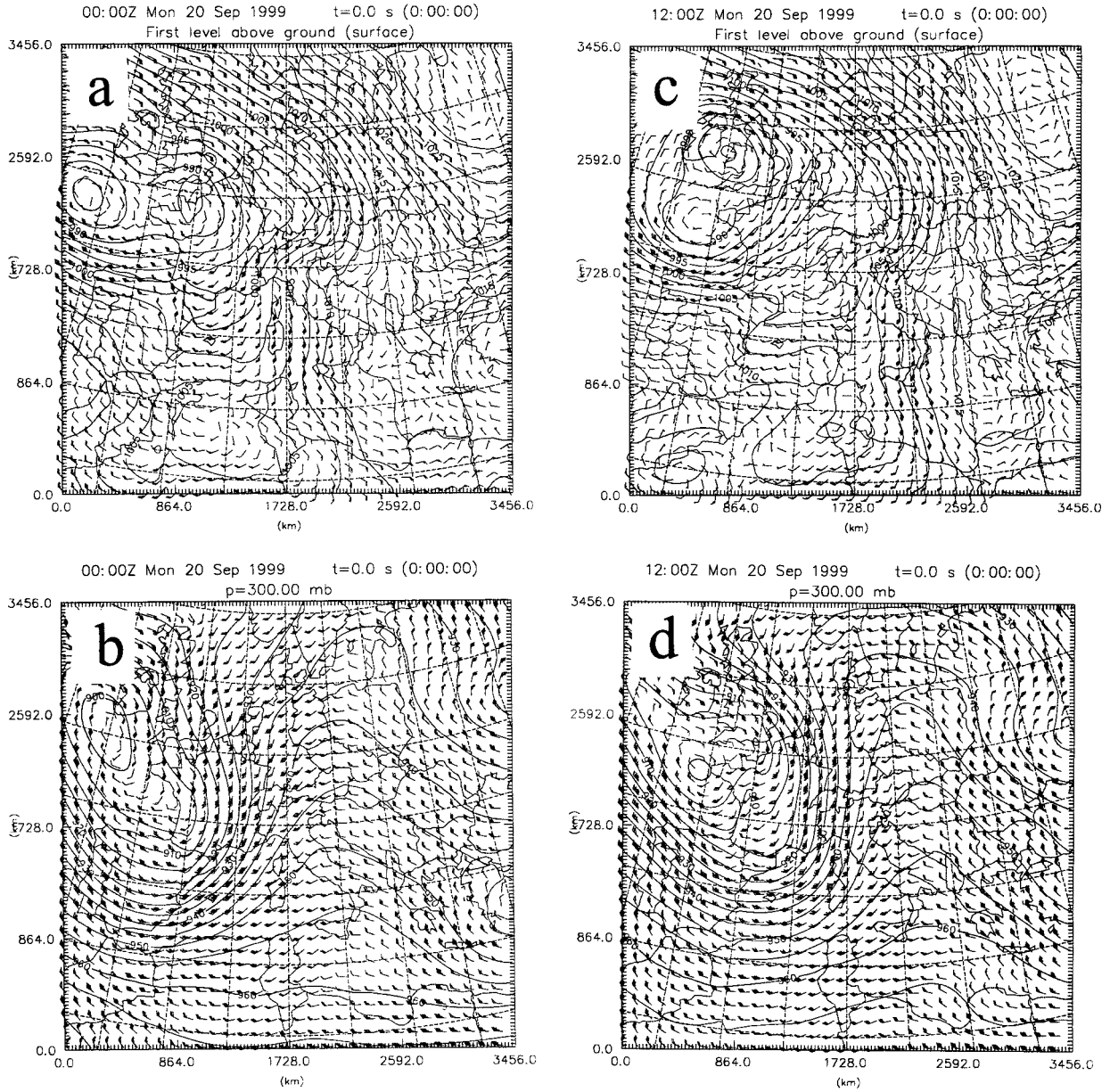

FIG. 9. NCEP reanalysis fields for MAP IOP2 on 20 Sep 1999: (a) surface at 0000 UTC, (b) 300 hPa at 0000 UTC, (c) surface at 1200 UTC, and (d) 300 hPa at 1200 UTC.

tionally or potentially unstable airstream impinging on the mountains, 2) a very moist LLJ, 3) steep mountains to help release the conditional instability, 4) an upper-tropospheric deep short-wave trough or high-PV (potential vorticity) anomaly approaching the threat area (which helps to enhance low-level upward motion), and 5) an upper-tropospheric quasi-stationary high pressure ridge to force the convective system to be quasi-stationary or slow its forward progress over the threat area. In addition, the low-level confluent flow plays an important role in helping to trigger the convection in the Alpine cases. For the MAP IOP2 case, a tongue of high moisture extended into the threat area. In the next section, we will examine whether or not these conditions are common for producing heavy orographic rainfall in east Asia.

4. Heavy orographic rainfall associated with tropical storms or depressions in east Asia

a. The heavy orographic rain event of 7 August 1999 in Taiwan

The Central Mountain Range of Taiwan has a length of about 300 km oriented in a north-northwest to south-southeast direction, a width of about 100 km, an average

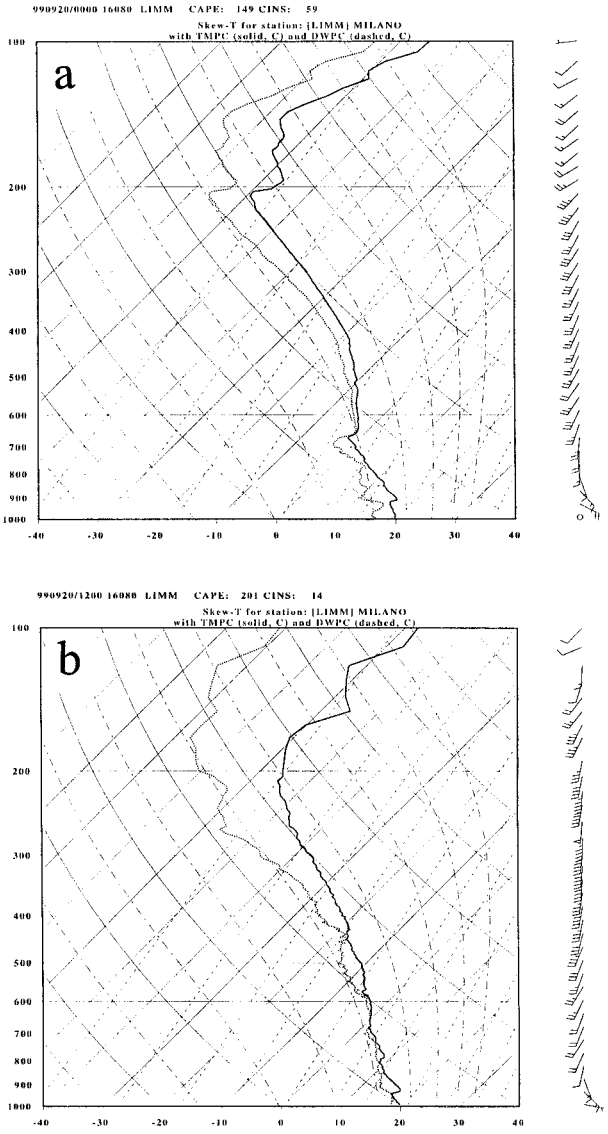

FIG. 10. Soundings observed at Milan, Italy, at (a) 0000 and (b) 1200 UTC 20 Sep 1999 for MAP IOP2 heavy rainfall event.

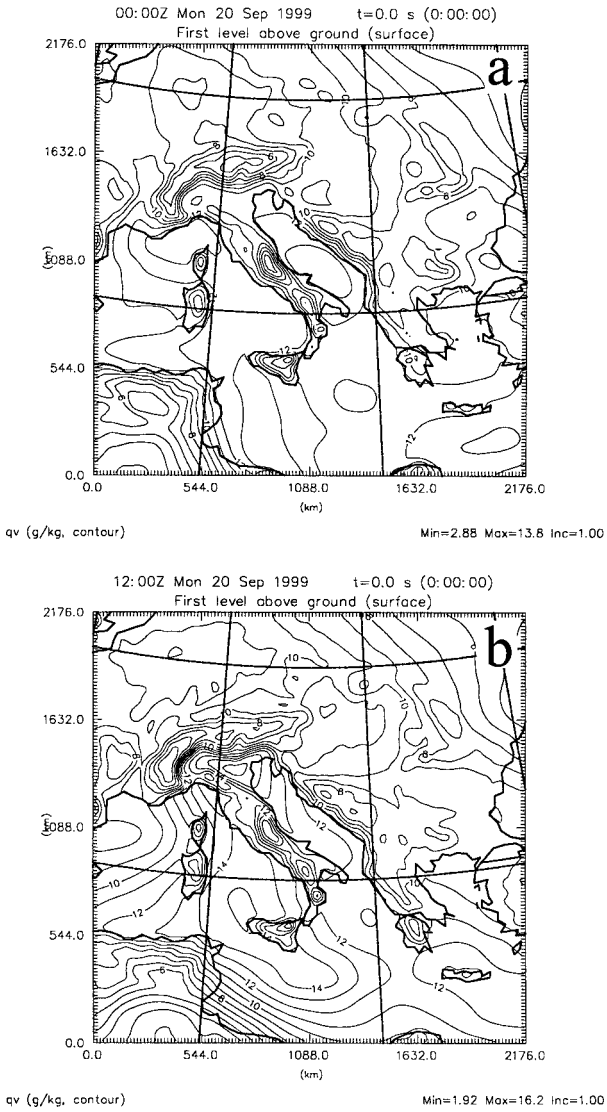

FIG. 11. Water vapor mixing ratio (in g kg^{-1}) for MAP IOP2 at (a) 0000 and (b) 1200 UTC 20 Sep 1999.

height of about 2.5 km, with the highest peak about 4 km (Fig. 12). Since the CMR is very high, extremely steep, isolated, and surrounded by oceans, it serves almost like a natural laboratory for studying the orographic effects on impinging airflow and weather systems (e.g., see the review by Lin 1993).

Tropical Storm (TS) Rachel approached Taiwan at 1200 UTC 6 August 1999 from the southwest passing over the Taiwan Strait (Fig. 13) and produced heavy rainfall on the southwest coast of Taiwan during the early morning (local time) of 7 August. The maximum accumulated rainfall in southwest Taiwan reached 347 mm for a 2-day period starting at 0000 UTC 6 August. Thus, this particular event provides a good case for examining the synoptic and mesoscale features responsible for producing heavy orographic rainfall, as found from the U.S. and Alpine events.

This tropical storm can also be seen clearly from the enhanced IR satellite imagery (Fig. 13). At 1200 UTC 6 August, the mesoscale convective system associated with the tropical storm covered a circular area with a diameter comparable to the meridional (north–south) extent of Taiwan (about 400 km). Some scattered convective clouds had already erupted before 0600 UTC 6 August (Fig. 13) over the CMR and also to the southwest of Taiwan. Since TS Rachel is located so far away at this time and the convection associated with it was strongest on its southwest side, it appears that *the convection was induced by the orographic lifting of the southwesterly conditionally unstable airflow. The low-level southwesterly flow was strengthened by the approaching tropical storm* (Figs. 15a,b and 16a,b). In other words,

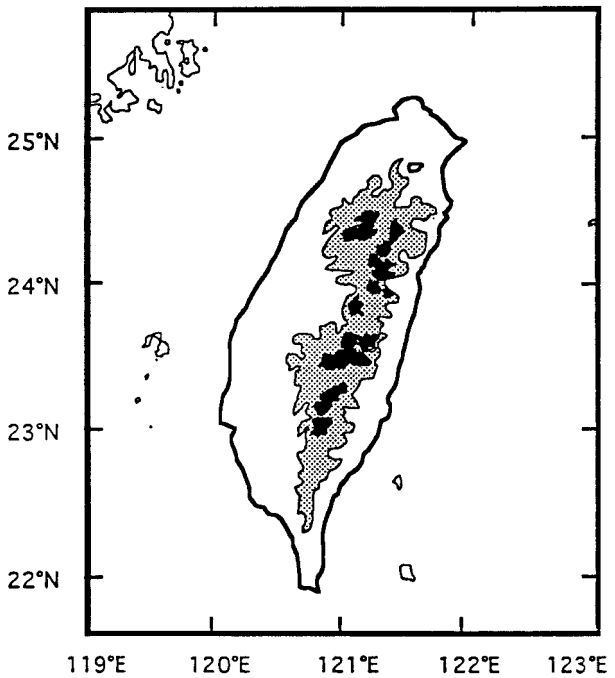

FIG. 12. Taiwan topography. The contour of 1 km is shaded and that of 3 km is darkened.

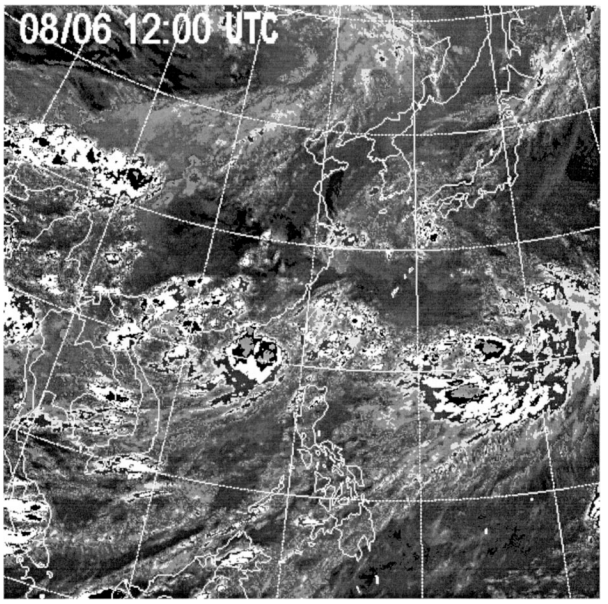

FIG. 13. The IR satellite images over East Asia for 1200 UTC 6 Aug 1999. Taiwan is located near the center of the figure.

a *significant amount of heavy rainfall was not directly associated with the convection embedded within the tropical storm.* At 1800 UTC 6 August, the convection located over the southwest coast of Taiwan increased significantly, while the strength of the convection to the northwest and east of the island remained about the same. The convection produced a maximum accumulated rainfall of more than 60 mm to the southwest and more than 20 mm to the northeast of Taiwan in a 6-h period (Fig. 14a). Note that the tropical storm was still about 500 km to the southwest of Taiwan at this time. By 0000 UTC 7 August, the whole island of Taiwan was covered by this convective system associated with the tropical storm (Fig. 13) and the 24-h accumulated maximum rainfall had reached about 160 mm (Fig. 14b).

In order to study the synoptic environment associated with the tropical storm and the orographic rainfall, we employ the Advanced Regional Prediction System, (ARPS; Xue et al. 2000) preprocessor to process the National Centers for Environmental Prediction's (NCEP) 2.5° reanalysis data. Figure 15 shows the surface pressure (Fig. 15a) and geopotential height fields (Figs. 15b–d) valid at 0000 UTC 6 August 1999. The tropical storm has a minimum central pressure of about 996 hPa and was located near (21.9°N, 117.9°E), about 500 km to the southwest of Taiwan. A southerly low-level jet, with a sustained maximum wind of about 18 m s^{-1}, was directed toward the southwest coast of Taiwan (Figs. 15a,b). The storm moved toward the west coast of Taiwan along an east-northeasterly track at a speed of about 5 m s^{-1}. The cyclonic circulation centered about 1700 km northeast of Taiwan is associated with Typhoon Paul. Other major surface synoptic features include a synoptic low located near Mongolia and a high located over the northwest Pacific Ocean (both are outside the plotting domain shown in Fig. 15). Typhoon Paul, which had a minimum central pressure of 990 hPa, forced TS Rachel to move slowly and cyclonically toward Taiwan. The slow movement of the tropical storm is important in producing long-lasting rainfall. AT 500 hPa, the tropical storm appeared to interact with Typhoon Paul (Fig. 15c). At 300 hPa, in additional to the tropical storm and Typhoon Paul (Fig. 15d), an upper-tropospheric low was located over the east coast of central China. This upper-level low may be identified as a cold-core low (CCL) due to its low temperature (not shown). It has been observed that CCLs play an important role in steering the typhoons over east Asia during the typhoon season (e.g., Kelly and Mock 1982). The CCL is often formed in the upper troposphere by a high to the west and a subtropical jet streak to the southeast. Similar to other CCLs, the present CCL has its maximum pressure gradient at 300 hPa and decreases in strength (intensity) both above and below this level. At 500 hPa, the CCL was weaker and had merged with Typhoon Paul to form a single system (Fig. 15c).

AT 1200 UTC 6 August 1999 (Figs. 16a,b), the low-level south-southwesterly flow turned more southwesterly, was strengthened by TS Rachel, and impinged more perpendicularly on the CMR, which forced the air to ascend to its level of free convection (LFC), which released the conditional or convective instability, and induced strong convection over the southwestern coast of the island, resulting in heavy rainfall. The effect of

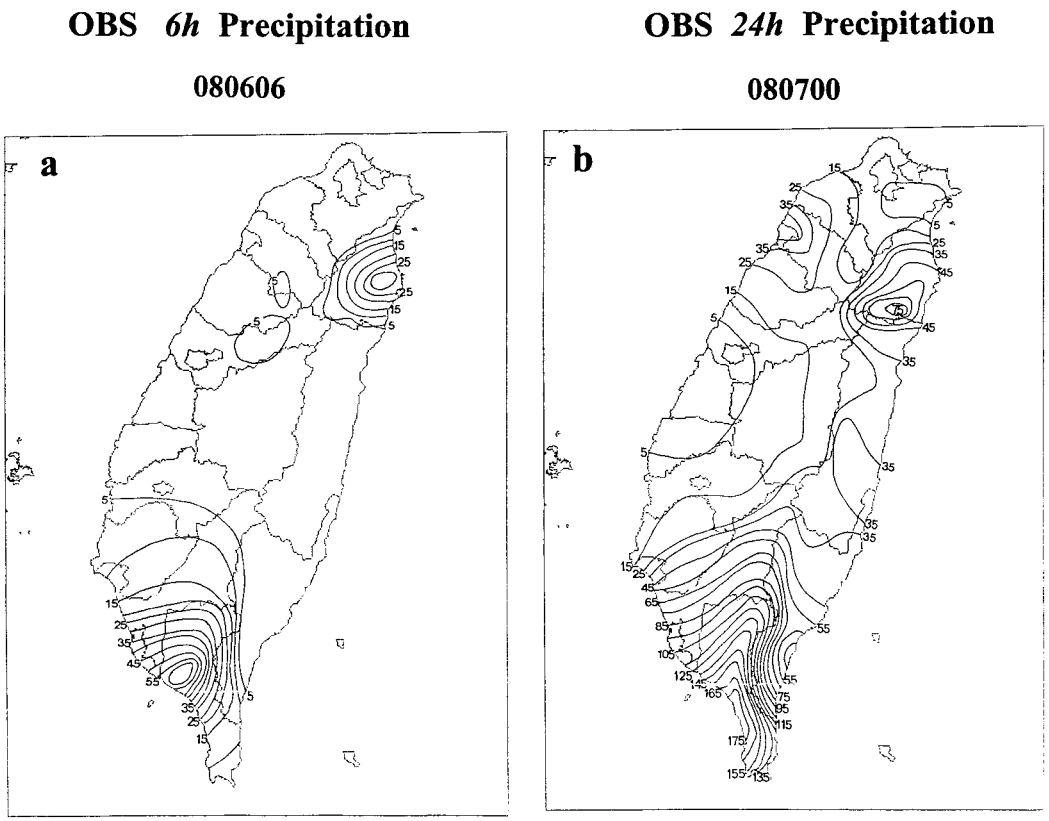

FIG. 14. Accumulated rainfall (in mm) over Taiwan from 0000 UTC 6 Aug to (a) 0600 UTC Aug, and (b) 0000 UTC 7 Aug 1999.

orographic lifting of the low-level air is evidenced by the upstream sounding at Tong-Kang (TKG) shown in Fig. 17, which gives an LCL of 0.2 km and an LFC lower than 0.6 km. Near the threat area, the CMR has a height of about 2 km. With such a strong LLJ of about 10 m s^{-1}, the low-level flow should have enough kinetic energy to climb up above the LFC and release the conditional instability. In addition to the orographic lifting, the concave geometry of the CMR near the threat area (southwest of Taiwan; see Fig. 14) appears to also generate confluent flow and enhance the upward motion, as is often observed in other cases of heavy orographic rain. The upstream flow has a very high CAPE (2099 J kg^{-1}) at this station (TKG; Fig. 17a). From the sounding at 0600 UTC 6 August, one also can see that the flow is very moist in the lower layer, which has a mixing ratio of about 21 g kg^{-1} and an 84% relative humidity near the surface. The TKG sounding (Fig. 17a) also indicates that the low-level flow (say, 1000–900 hPa) is potentially unstable since $\partial\theta_e/\partial z < 0$. *Thus, the tropical storm played a role in enhancing the southwesterly low-level jet, transporting the conditionally and potentially unstable air to the threat area, which allowed the mountains to force the air upward and release the instability.*

b. The flood of 7 August 1959 in Taiwan

During the evening of 7 August 1959, a tropical depression approached Taiwan from the southwest, which resulted in severe orographic rainfall and flash flooding over southern and central Taiwan. This flooding caused 665 deaths and 425 missing people, left 250 000 people homeless, resulting in an economic loss of $100 million (U.S.); caused to rivers overflow; left 62% of the country's farms partially or completely submerged under the flood water; and damaged bridges, railroads, and highways, causing significant interruptions to private and commercial traffic. Due to the similarities between the synoptic and mesoscale environments in this case and those of the 1999 heavy orographic rainfall event, a comparison of these two events may help to identify the common synoptic and mesoscale environmental features for this type of heavy orographic rainfall event.

Our discussion of the synoptic situation will also be based on the 2.5° NCEP reanalysis dataset, processed by the ARPS preprocessor (Xue et al. 2000). At 0600 UTC 6 August 1959, a tropical depression was located to the southeast of China and was located approximately 400 km west-northwest of Taiwan (Fig. 18a). Concurrently, Typhoon Ellen was located to the north-northeast of Taiwan, south of Korea, and southwest of Japan.

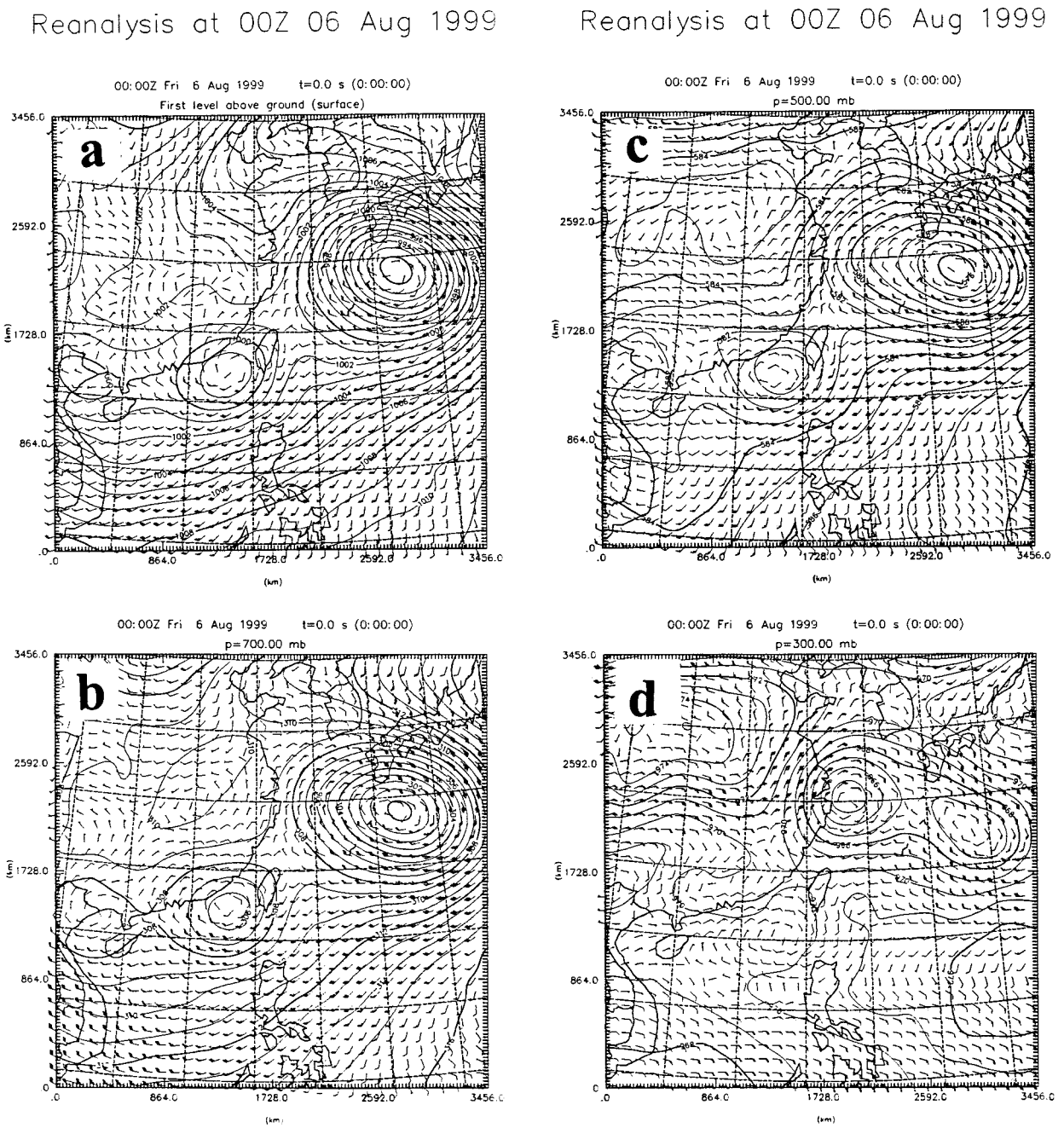

FIG. 15. NCEP reanalysis data over east Asia valid at 0000 UTC 6 Aug 1999: (a) surface vector wind (m s^{-1}) and sea level pressure (hPa), and combined vector wind and geopotential height (m) fields at (b) 700, (c) 500, and (d) 300 hPa.

From the synoptic charts (not shown), one also can identify a low pressure system located to the northeast of Typhoon Ellen, with the Pacific high located farther to the northeast of the low. Thus, the synoptic situation at the surface is very similar to that of the 1999 heavy orographic rain event in Taiwan except that the tropical depression is much weaker in this case. On the other hand, the synoptic situation in the mid- and upper troposphere is significantly different from the 1999 case. At the 700-hPa surface (Fig. 18b), the strong cyclonic circulation associated with Typhoon Ellen and the cyclonic circulation associated with the tropical depression dominated the flow field. The circulation center associated with the tropical depression was located close to the position of the surface low.

At both the 500- and 300-hPa surfaces (Figs. 18c,d), the flow fields were much simpler compared to the 1999 case. In the present (1959) case, they were basically

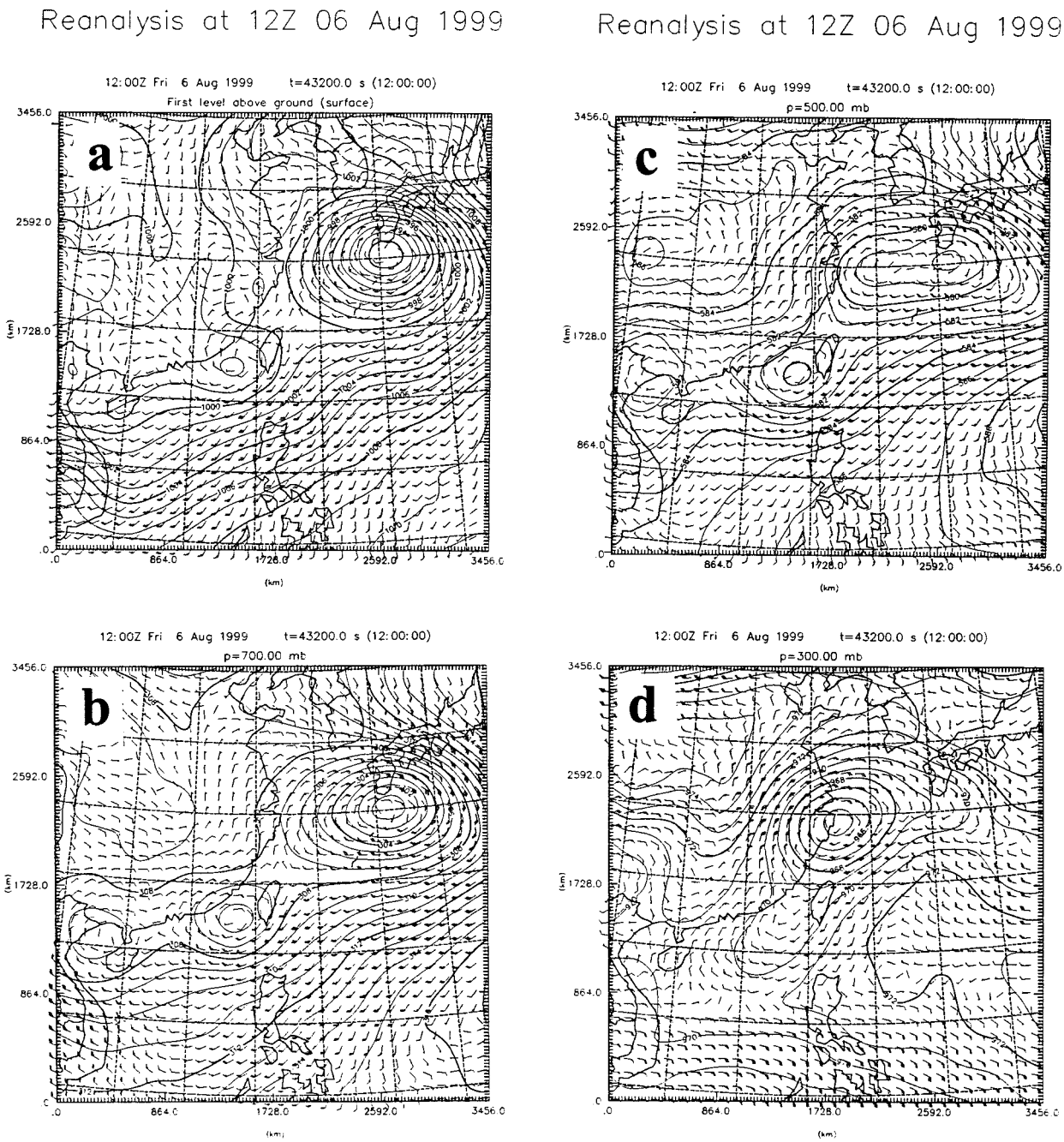

FIG. 16. Same as in Fig. 15 except valid at 1200 UTC 6 Aug 1999.

dominated by Typhoon Ellen and a low associated with the tropical depression over southeast China. Similar to the 1999 case, the tropical depression did play a role in enhancing the low-level jet impinging on the southwestern CMR. In addition, even though the tropical depression was still more than 400 km away from Taiwan, rain had already started falling along the southwest coast (Fig. 19a). The southwesterly LLJ had a velocity of about 17.5 m s^{-1} at TKG (Tong-Kang, an upstream location) at 0000 UTC 7 August and flowed almost perpendicularly to the CMR, which provided strong uplift to the incoming airstream. The southwesterly flow was very moist, conditionally unstable, and as can be seen from the sounding around this time (Fig. 20), had a mixing ratio of 22 g kg^{-1} and CAPE values as high as 2406 J kg^{-1} at 0000 UTC 7 August. The lower-layer (e.g., say 1000–900 hPa) flow is also potentially unstable since $\partial\theta_e/\partial z < 0$ (Fig. 20a).

At 0600 UTC [1400 local standard time (LST)] 7 August 1959, approximately 3 h prior to the occurrence

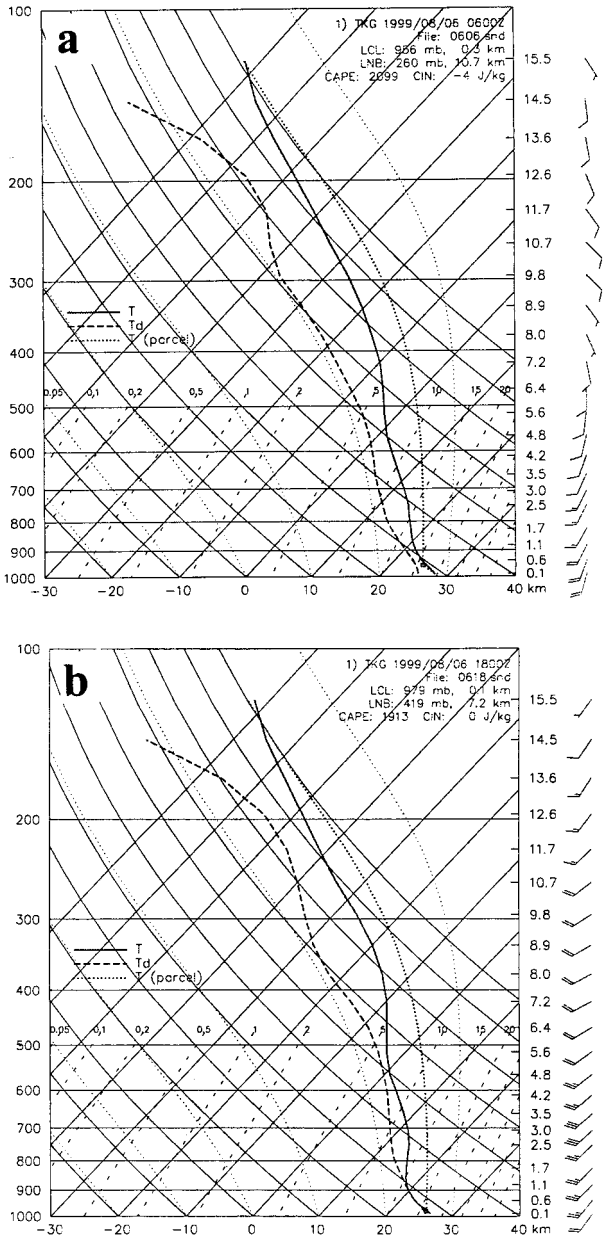

FIG. 17. Soundings at an upstream location of Taiwan's CMR (Tong-Kang) at (a) 1200 and (b) 1800 UTC 6 Aug 1999. One full bar denotes wind speed of 10 kt (about 5 m s^{-1}).

of the heavy rainfall, the tropical depression weakened, and could no longer be detected at the surface (Fig. 21a), but could still can be detected in the 700- and 500-hPa reanalysis fields (Figs. 21b and 21c). A closed circulation can still be identified from the 700-hPa chart. The magnitude of the low-level jet remained about 17.5 m s^{-1}, similar to the maximum low-level wind values during the previous 24 h as Typhoon Ellen moved slightly closer to the southwest of Japan. It appears that Typhoon Ellen was able to help slow the movement of the tropical depression as well as force the center of the tropical depression to turn counterclockwise with respect to Typhoon Ellen, similar to what Typhoon Paul did to the tropical storm of 7 August 1999. At 300 hPa (Fig. 21d), the circulation in between Taiwan, China, Korea, and Japan was dominated by Typhoon Ellen. The cyclonic circulation associated with the tropical depression over southeastern China during the previous 24 h became an anticyclonic high, which appeared to be associated with the upper-level outflow of the tropical depression. This anticyclonic circulation might have interacted with Typhoon Ellen to produce stretching deformation, leaving a confluent flow field over the west coast of Taiwan at 300 hPa, where heavy rainfall occurred. This is detrimental to the development of low-level vertical motion ($w > 0$). While the effects of this upper-tropospheric anticyclonic circulation on the low-level vertical motion need further investigation, the low-level flow seemed to be able to overcome this and produced heavy rainfall over the west coast of Taiwan. The synoptic and mesoscale situations during most of 8 August (not shown) were similar to those of 7 August, particularly the low-level jet, which was able to help maintain the rainfall continuously throughout the period from 0900 UTC 7 August to 0000 UTC 8 August. During this period of heavy rainfall, a wide area in the western and southwestern parts of Taiwan had an average rainfall of 1000 mm (Fig. 19b). The local maximum rainfall total reached 1000 mm within 16 h. The heavy rainfall decreased significantly after 1800 UTC 8 August (0200 LST 9 August) due to the filling of the tropical depression and the weakening of the southwesterly low-level jet (not shown). Compared to the 1999 case, the rainfall was much heavier, which may be explained by the stronger LLJ and larger CAPE, even the tropical depression was weaker.

c. A heavy orographic rain event in Kyushu, Japan

In this section, we will briefly review a heavy rainfall event, which occurred over southeastern Kyushu, Japan, on 29–30 August 1974, following Sakakibara (1979). Similar to the Taiwanese cases discussed above, the heavy rainfall was induced by the Kyushu mountain range affecting/influencing a strong southeasterly LLJ associated with an approaching tropical depression. The major mountain range of Kyushu (the southernmost island of Japan), that is, the Kyushu Sanchi, is oriented approximately parallel to the coast, that is, roughly in a north-northeast to south-southwesterly direction (Fig. 22b). The highest peak of the mountain range is higher than 1500 m and the slope is approximately 1/50.

At 1200 UTC (2100 LST) 29 August 1974, a tropical depression approached Kyushu from the southeast. The major synoptic features at this time are shown on the 850-hPa map (Fig. 22a) and depicted by the flow fields at the surface, and 700, 500, and 300 hPa (Fig. 23). Again, the ARPS (Xue et al. 2000) preprocessor has processed these NCEP analyzed fields. A cyclone was

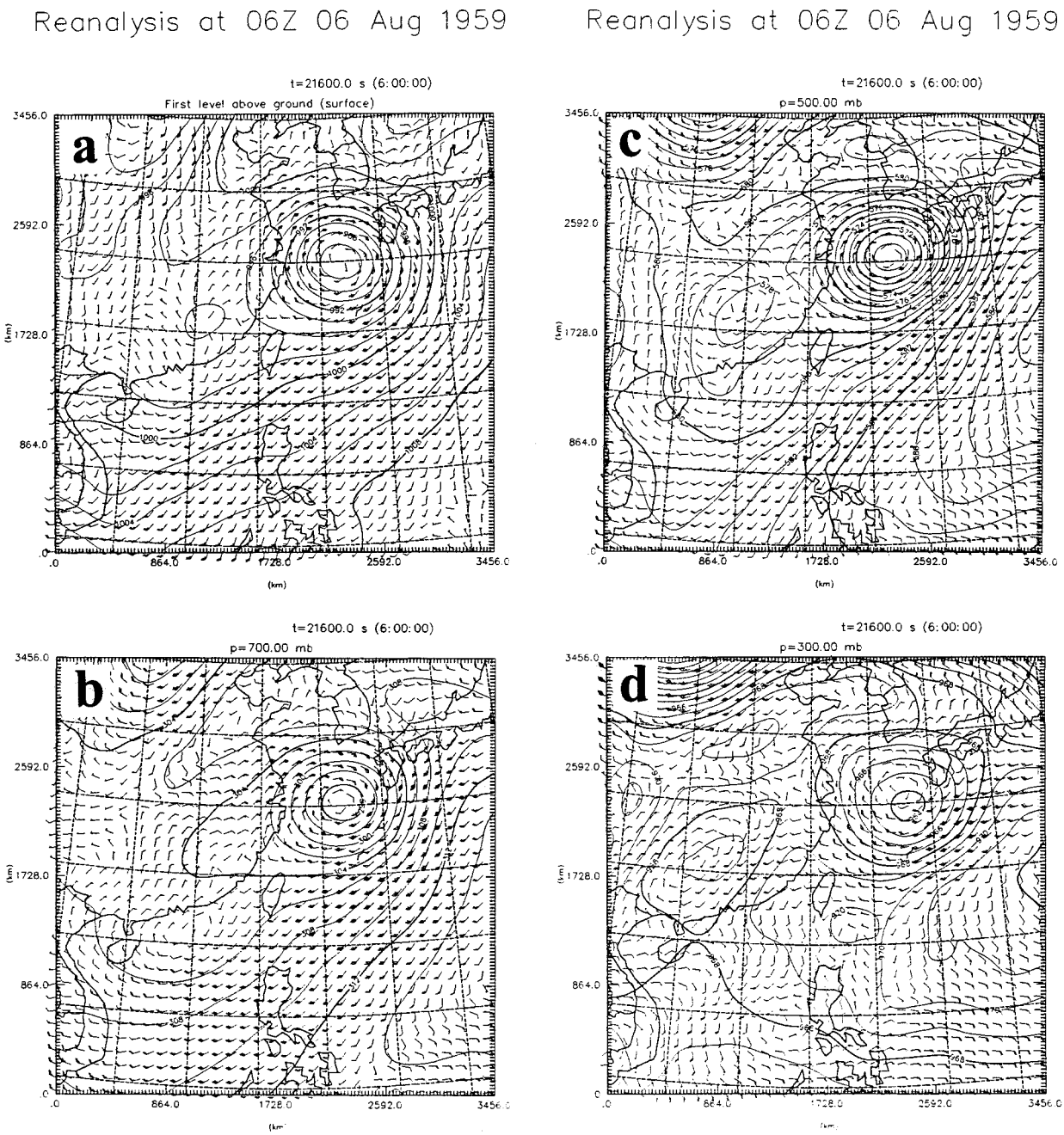

FIG. 18. NCEP reanalysis data over east Asia for (a) surface, and (b) 700, (c) 500, and (d) 300 hPa at 0600 UTC 6 Aug 1959.

located to the south of the Korean peninsula (Figs. 22a and 23a). This cyclone tilted westward with height, which is typical for an extratropical cyclone. A cold front extended roughly southward from the cyclone, as can be seen clearly from the satellite images (Figs. 22c and 22d). A warm front extended east-northeastward from this extratropical cyclone over the Japan (East Korean) Sea. This cyclone–front system was quasi-stationary during the heavy rainfall period, which was important in producing relatively long-lasting precipitation over the Kyushu mountain range. In addition to the tropical depression, extratropical cyclone, and frontal system, another weaker tropical depression was located south of Kyushu and west of the major tropical depression (Fig. 22a). This weaker tropical depression decreased in strength (intensity) from 1200 UTC 29 August to 0000 UTC 30 (Figs. 22c and 22d; Fig. 23). On the 300-hPa surface, a jet streak was located to the east of the extratropical cyclone and an anticyclonic circulation was located in between the major tropical de-

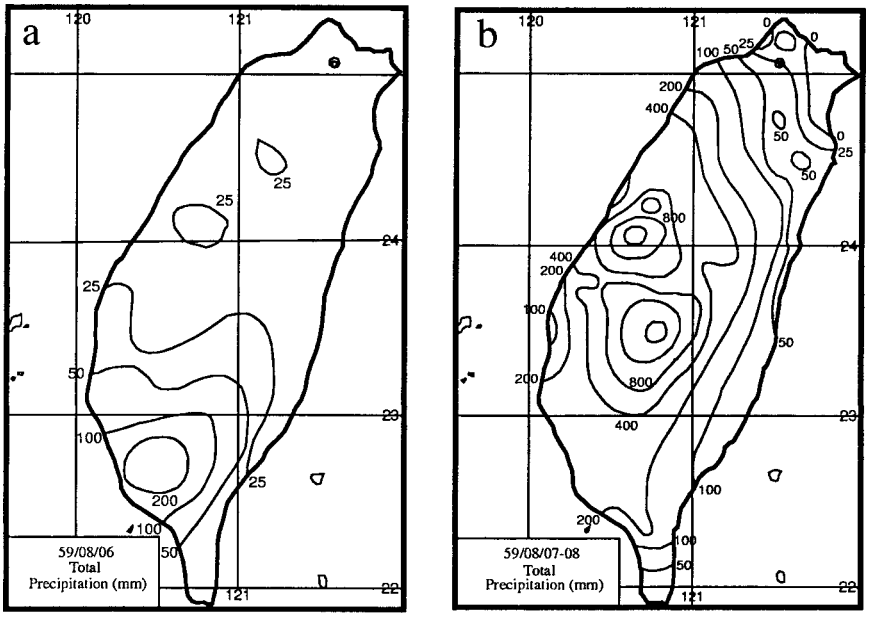

FIG. 19. Accumulated rainfall (in mm, solid curves) over Taiwan for (a) 6 Aug (1 day), and (b) 7 and 8 Aug (2 days) 1959.

pression and the stationary front (which might have been induced by these two systems, i.e., the tropical depression and the stationary front). Similar to the 1959 Taiwanese case and unlike the 1999 Taiwanese case, there were no other significant synoptic features that existed in the upper troposphere.

It is important to mention that from the IR satellite image valid at 1200 UTC (2100 LST) 29 August (Fig. 22c), there was no thick, massive cloud cover over or in the vicinity of the Japanese Islands. However, from the visible satellite image valid at 0000 UTC (0900 LST) 30 August (Fig. 22d), a cluster of small clouds started to form along the Pacific coast of the Japanese Islands, even though the tropical depression was still located several hundred kilometers off the coast. Apparently, these clouds were formed by convection triggered by the interaction of the mountain and the southeasterly moist, potentially unstable low-level jet associated with the tropical depression (Sakakibara 1979). In other words, the tropical depression plays a role similar to those present in the Taiwanese cases described earlier, which helped produce heavy orographic rainfall on the upstream and upslope side of the Kyushu mountains. According to Sakakibara (1979), the echoes observed by the Tanegashima radar at 3-h intervals from 0400 UTC (1300 LST) 29 August to 0600 UTC (1500 LST) 30 August 1974 are restricted from the windward (southeastern) slope of the mountain range out into the ocean, approximately 150 km off the coast of Kyushu Island (not shown). The maximum intensity was located over the windward slope and the intensity of echoes sharply decreased near the crest of the mountain range. Similar to the Taiwanese cases, this implies that the heavy rainfall was induced by the mountains at this time, instead of being associated with the convection which had already existed within the tropical depression. The maximum daily rainfall reached an amount greater than 150 mm (Sakakibara 1979).

Similar to the Taiwanese cases, the upslope convection was triggered by orographic lifting of the LLJ impinging on the Kyushu mountain range. The southeasterly low-level wind was enhanced by the cyclonic circulation associated with the major tropical depression that approached Kyushu Island, and resulted in a low-level jet with a velocity of about 17.5 m s^{-1} upstream of the Kyushu mountains (Figs. 22a and 23a). The CAPE at Shinomisaki (Shin, an upstream station) at this time (1200 UTC 28 Aug) was 1149 J kg^{-1}, as revealed by an analysis of the sounding data. Note that this LLJ was oriented almost perpendicular to the Kyushu mountains. Figure 24 also shows that the air upstream of the Kyushu mountains has high CAPE (Fig. 24b) as well as a high water vapor mixing ratio (Fig. 24a).

d. Common synoptic and mesoscale features responsible for heavy orographic rain induced by a tropical storm or depressions in Taiwan and Japan

Based on the above discussions, we may conclude that the following synoptic and mesoscale features are common for producing heavy orographic rainfall associated with a tropical storm or depression in Taiwan and Japan: 1) A steep mountain helps to release the conditional or convective instability. 2) A tropical storm or depression helps to induce the LLJ. 3) The LLJ is

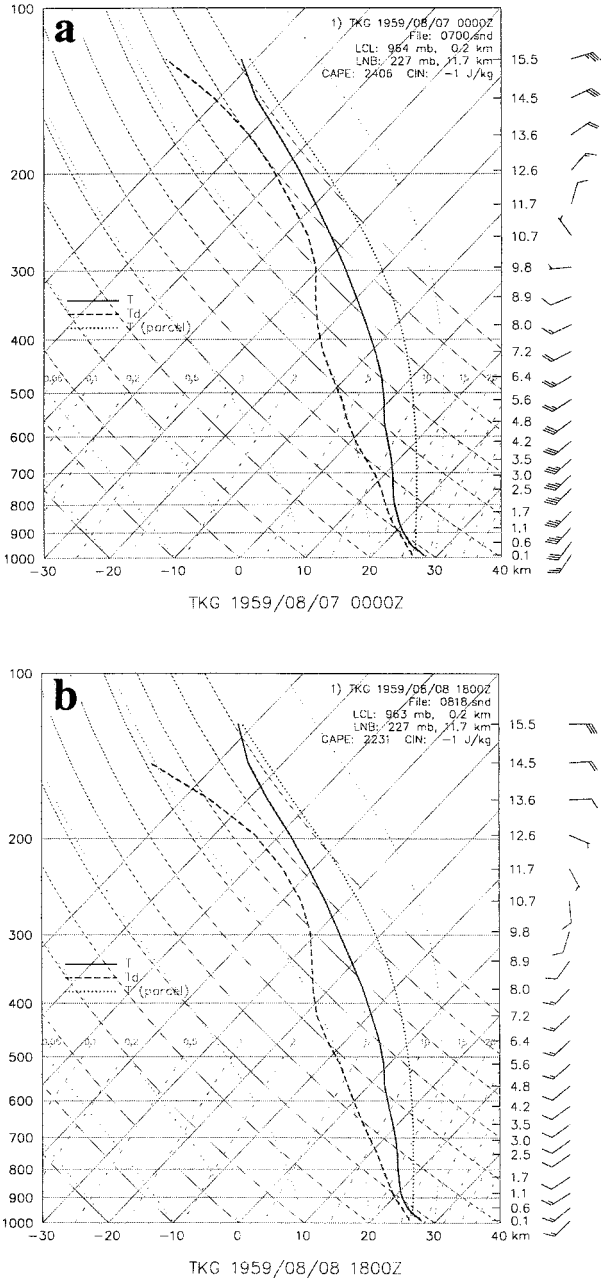

FIG. 20. Soundings at an upstream location (Tong-Kang) of Taiwan's CMR at (a) 0000 UTC 7 Aug and (b) 1800 UTC 8 Aug 1959.

highly conditionally (i.e., high CAPE) and potentially unstable. 4) A quasi-stationary synoptic system, such as a typhoon in Taiwanese cases or a stationary front in Japanese cases, acts to impede or slow the movement of the convective system over the mountains.

5. Some common ingredients for producing heavy orographic rainfall

From sections 2 and 3, it appears that there exist some common synoptic and mesoscale environments conducive to heavy orographic rainfall in the United States, European Alps, Taiwan, and Japan. These environments typically contain features such as conditionally or potentially unstable airflow accompanying an LLJ, high mountains, and quasi-stationary synoptic-scale systems. On the other hand, some features are not shared by all events, such as the high values of CAPE observed in both the Japanese and Taiwanese cases.

In order to better understand the dynamical basis for the observed common synoptic and mesoscale features, we may extend the ''ingredients-based methodology'' proposed by Doswell et al. (1996) to the situation of heavy orographic rainfall. Based on Doswell et al., the heaviest precipitation occurs where the rainfall rate is the greatest for the longest period of time. Thus, if R is the average rainfall rate and D is the duration, then the total precipitation produced, P, is determined by

$$P = RD \tag{1}$$

Here we are interested in flash flooding, which results from high to extremely high rainfall rates, instead of prolonged flooding, such as that produced by overrunning lakes and rivers. The rainfall rate can then be determined by the precipitation efficiency, E, and the vertical moisture flux, wq,

$$R = E(wq). \tag{2}$$

Substituting Eq. (2) into Eq. (1) leads to

$$P = E(wq)D. \tag{3}$$

The duration of heavy rainfall may be estimated by

$$D = L_s/c_s, \tag{4}$$

where L_s and c_s are the horizontal scale of the convective system and its propagation speed in the direction of the system movement, respectively. Combining Eqs. (3) and (4) yields

$$P = E(wq)L_s/c_s. \tag{5}$$

Thus, if one of, or any combination of the factors on the right-hand side is large while the others are at least moderate in size, then there is a potential for heavy rainfall. Based on Eq. (5), Doswell et al. (1996) proposed the essential ingredients for flash floods over a flat surface. The precipitation efficiency is mainly controlled by microphysical processes, which are often difficult to measure or estimate. In addition, the presence or absence of vertical wind shear may also influence the precipitation efficiency. For flow over a mountain range, the low-level upward vertical motion may be controlled by either orography or the environment (e.g., upper-tropospheric divergence),

$$w = w_{\text{oro}} + w_{\text{env}}. \tag{6}$$

The orographically forced upward vertical motion may be roughly estimated by the lower boundary condition for flow over orographic terrain,

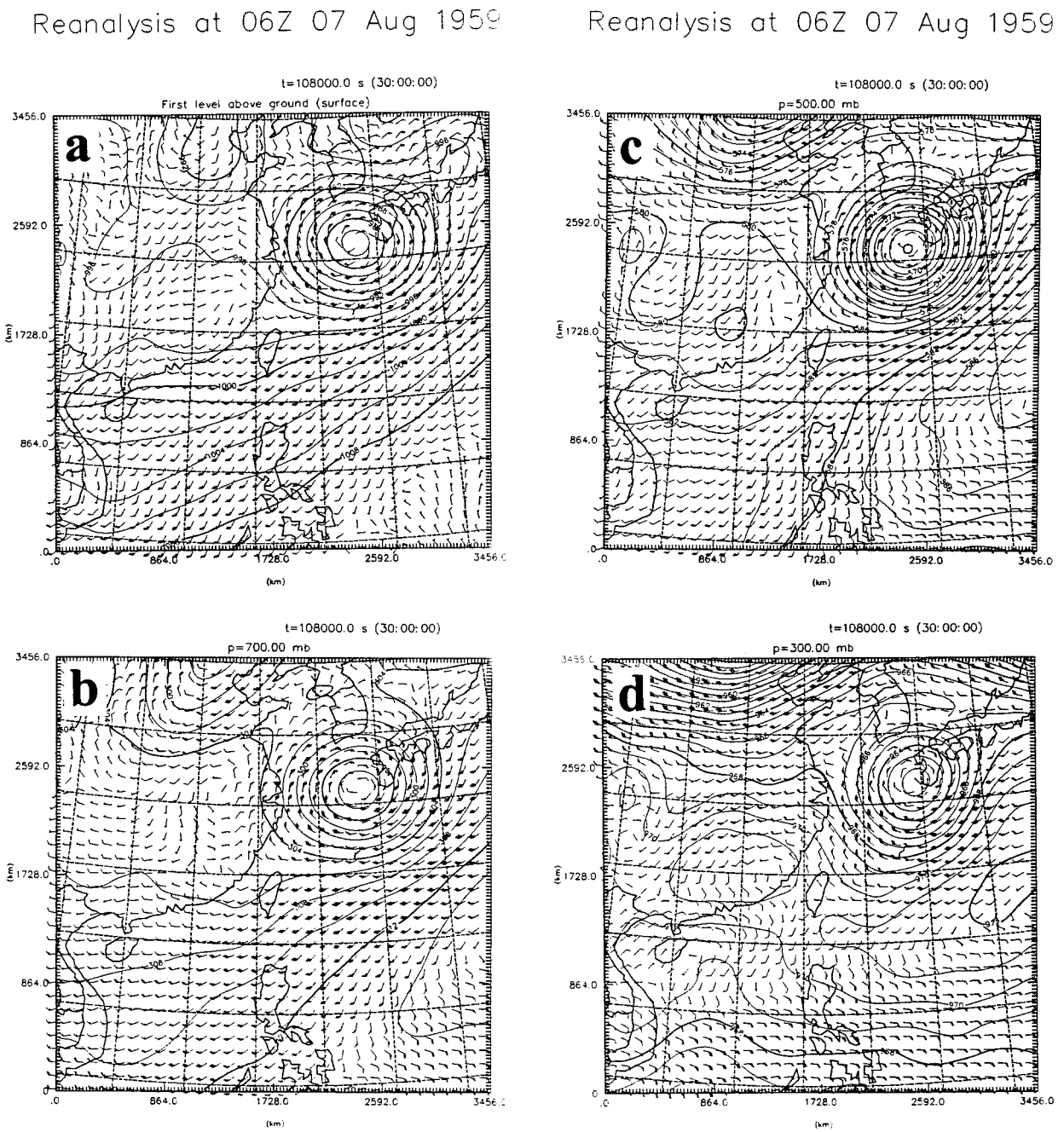

FIG. 21. Same as in Fig. 18 except at 0600 UTC 7 Aug 1959.

$$w_{\text{oro}} = \frac{Dh}{Dt} = \mathbf{V}_H \cdot \nabla h, \tag{7}$$

where $h(x, y)$ is the mountain geometry and $\mathbf{V}_H$ is the total low-level horizontal wind vector. The environmentally forced upward vertical motion (w_{env}) is determined by the transient synoptic setting, such as the divergence associated with an approaching deep shortwave trough in the U.S. and Alpine cases. Combining Eqs. (5), (6), and (7) gives

$$P = E(\mathbf{V}_H \cdot \nabla h + w_{\text{env}})qL_s/c_s. \tag{8}$$

Alpert (1986) and Doswell et al. (1998) have used a form similar to $\mathbf{V}_H \cdot \nabla h$ to diagnose three episodes of heavy rainfall in the western Mediterranean. Note that in general, w may not simply be decomposed (i.e., partitioned) into environmentally and orographically forced parts, since they are linked nonlinearly. *However, if* $\mathbf{V}_H$ *is measured at a time and location close to the occurrence of the event, then the nonlinear contribution from*

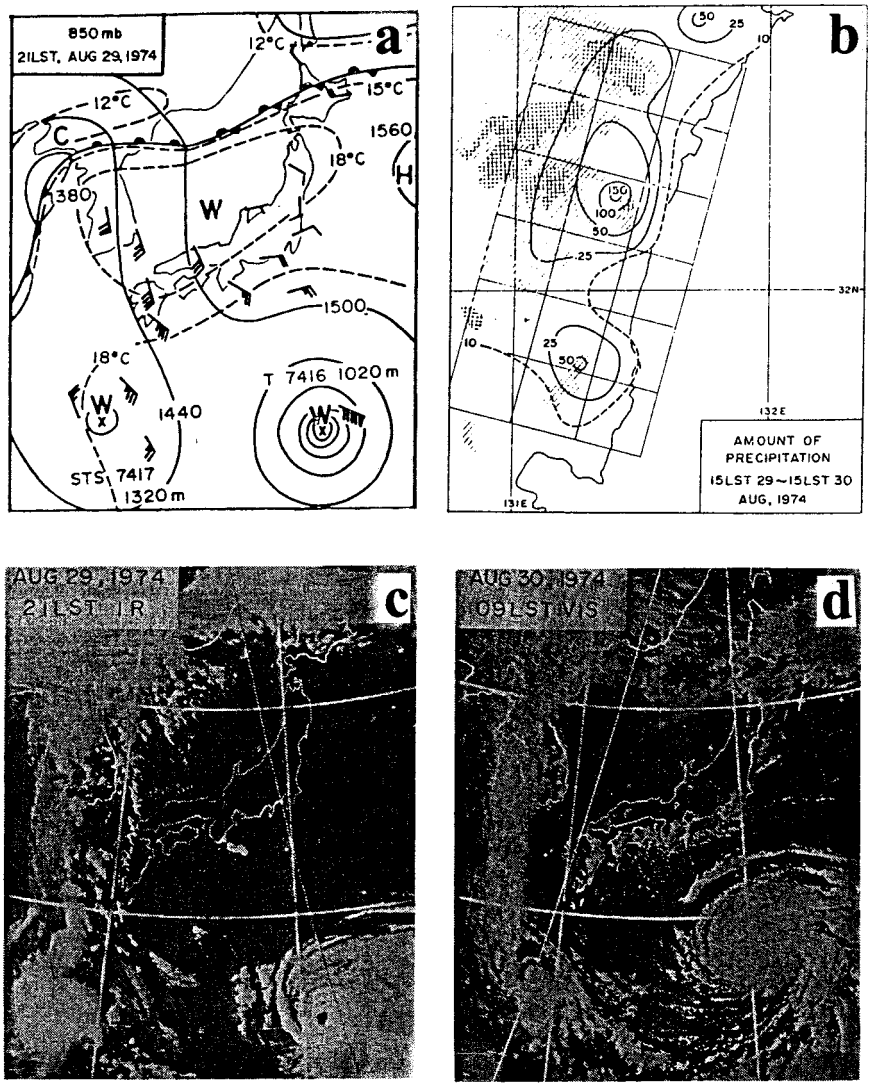

FIG. 22. (a) Synoptic situation at 1200 UTC (2100 LST) 29 Aug 1974 depicted by 850-hPa map around the Japanese Islands. The solid and dashed lines represent geopotential height at 60-m intervals and temperature at 3°C intervals, respectively. A full barb denotes 10 kt (~5 m s^{-1}) of the wind. (b) Daily amount of precipitation. Solid lines are isopleths of the daily amount of precipitation at 25-mm intervals. The hatched and cross-hatched shadings depict the areas higher than 500 and 1000 m, respectively. (c) Infrared image with lower resolution taken at 1200 UTC 29 Aug 1974. (d) Visible image with higher resolution taken at 0000 UTC (0900 LST) 30 Aug 1974. [After Sakakibara (1979).]

the approaching synoptic system (such as an approaching short-wave trough) *to* w_{oro} *will be partially contained in* $\mathbf{V}_H$. Besides the ingredients included in Eq. (8), a conditionally or potentially unstable airstream is also needed to help trigger deep convection (e.g., Doswell et al. 1996), a feature that is always observed in cases of heavy orographic rainfall. Therefore, we may conclude that a heavy orographic rainfall requires significant contributions from any combination of the following common ingredients: 1) high precipitation efficiency of the incoming airstream (large E), 2) an intense low-level jet (large $\mathbf{V}_H$), 3) steep orography (large ∇h), 4) favorable (i.e., concave) mountain geometry and a confluent flow field (large $\mathbf{V}_H \cdot \nabla h$), 5) strong synoptically forced upward vertical motion (large w_{env}), 6) a high moisture flow upstream (large q), 7) the presence of a large, preexisting convective system (large L_s), 8) slow (impeded or retarded) movement of the convective system (small c_s), and 9) a conditionally or potentially unstable low-level flow, (required to trigger deep convection). According to Doswell et al. (1996), precipitation efficiency typically does not play an important role in producing heavy rainfall unless there is reason to believe that it will be unusually low, such as for high-

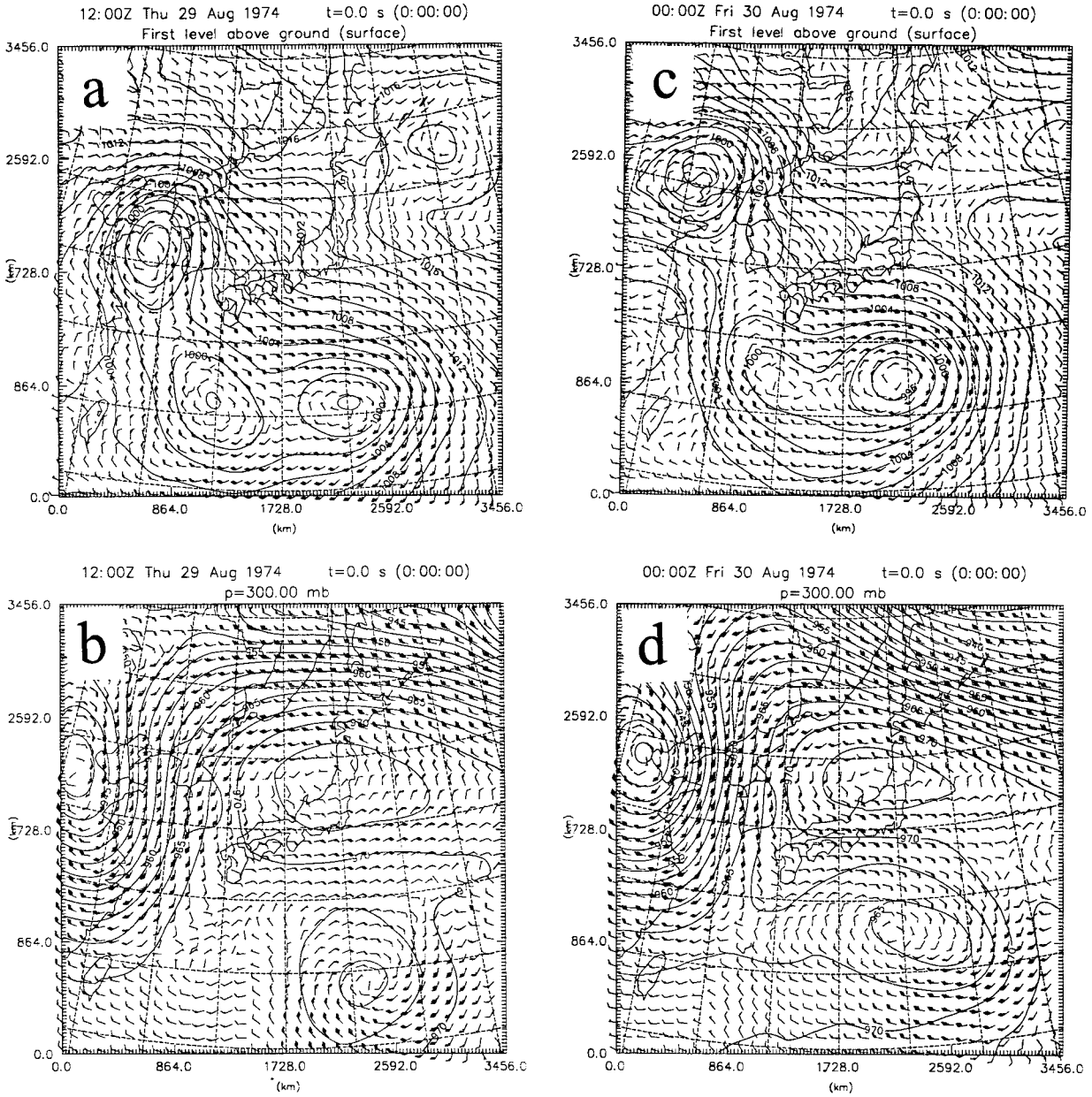

FIG. 23. NCEP reanalysis fields: (a) surface at 1200 UTC 29 Aug, (b) 300 hPa at 1200 UTC 29 Aug, (c) surface at 0000 UTC 30 Aug, and (d) 300 hPa at 0000 UTC 30 Aug 1974.

based convection over the interior of a mountain range. The moisture content may be represented either by the water vapor mixing ratio or by the amount of precipitable water in a vertical column of air (see, e.g., Saucier 1955). This may be done conveniently by using a thermodynamic chart, such as the skew T–log$p$ diagram.

Thus, the common synoptic and mesoscale conditions conducive to heavy orographic rainfall over U.S. and Alpine orography, as discussed in sections 2 and 3, belong to a subset of the above-listed common ingredients. Although a high CAPE value is not consistently observed for U.S. and Alpine heavy orographic rainfall events (based on sounding data), this remains to be investigated due to the highly inherent temporal and spatial variations typically associated with such data. For Alpine heavy orographic rainfall events, which often start in a concave region (such as the Ticino region in Switzerland and the Lago Maggiore region in Italy), mesoscale vertical motion may be produced if there exists incoming confluent flow as indicated by ingredient 4. Similarly, the common synoptic and mesoscale conditions found in Taiwanese and Japanese cases can be explained by the common ingredient argument, as discussed above. Note that the typhoons and stationary

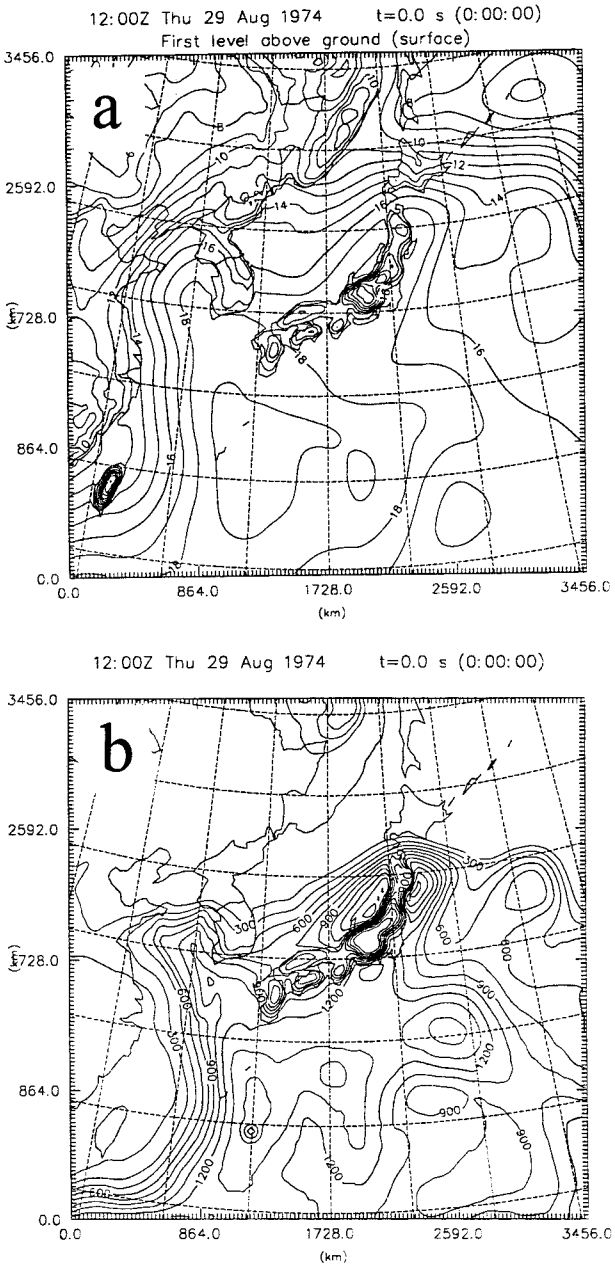

FIG. 24. (a) Water vapor mixing ratio and (b) CAPE at 1200 UTC 29 Aug 1974 processed by ARPS preprocessor of the NCEP reanalysis data.

fronts play the role of quasi-stationary synoptic systems in the Taiwanese and Japanese cases, respectively, to slow the movement of the convective system over the mountains. In both these cases, the incoming airstream was maritime in nature (i.e., origin), and able to obtain a high content of moisture and high values of CAPE. This may also explain why no midtropospheric shortwave trough is needed to enhance the low-level upward vertical motion, such as that observed in both the U.S. and Alpine cases.

The above concept of common ingredients for producing heavy orographic rainfall may also be applied to events occurring in other regions or locations around the world. For example, the extreme precipitation (>500 mm in 1.5 days) event that occurred over New Zealand on 27 December 1989 developed when a deep layer of moist subtropical air along a cold front ascended the high terrain of South Island (Fig. 25). The intense orographic ascent was associated with an LLJ core with a maximum wind speed of over 20 m s^{-1} (Katsfey 1995). In addition, there was an upper-level trough and jet streak entrance region located upstream of South Island before the onset of heavy orographic rain. It is clear that the deep moist layer and LLJ are very helpful in producing heavy orographic rainfall. The upper-level trough and jet streak entrance region also provided additional forcing to induce low-level upward vertical motion, which satisfies ingredient 5. The synoptic low located to the southwest of South Island provided the necessary forcing to impede the progress of the convective system over the mountains since it moved very slowly southeastward (Fig. 25).

Another example is the Sichuan, China, flood, which occurred during the period from 11 to 15 July 1981 (Kuo et al. 1986). The synoptic situation included a strong southerly monsoon flow near the Sichuan basin, the passage of a deep midlatitude trough from the Lake Baikal region, and the formation of a long-lived mesoscale vortex near the Sichuan basin (Fig. 26). These conditions apparently satisfy some of the above-listed common ingredients for producing heavy orographic rainfall. The southerly monsoon flow provided very moist air, while the lee vortex enhanced the low-level jet. Although not emphasized in their paper, Fig. 26 does clearly show that there was a synoptic-scale high pressure system located to the east of the Sichuan basin, which was almost quasi-stationary and apparently provided the forcing necessary to slow down (impede) the movement of the convective system on the eastern flank of the Tibetan Plateau.

Figures 27a–c show the convective precipitation over the Western Ghats of India and the eastern Arabian Sea from 23 to 25 June 1979. The convective system produced a precipitation rate of 100–200 mm day^{-1}. In addition to the importance of the interaction between latent heating and the basic flow (e.g., Smith and Lin 1983), Ogura and Yoshizaki (1988) found that the presence of a strong low-level westerly jet, sheared environment, and latent and sensible heat fluxes from the ocean are essential. Clearly, the LLJ and high moisture in the low-level flow provided some common ingredients for producing the heavy orographic rainfall. In addition, for this particular case, the wind reversal level at about 5 km (Fig. 27d), at which the low-level westerly flow becomes easterly, is a critical level. A critical level is defined as the level at which the horizontal wind speed (U) equals the propagation speed (c) of the disturbance (wave); that is, $U = c$. (Note that $U = 0$ for a stationary

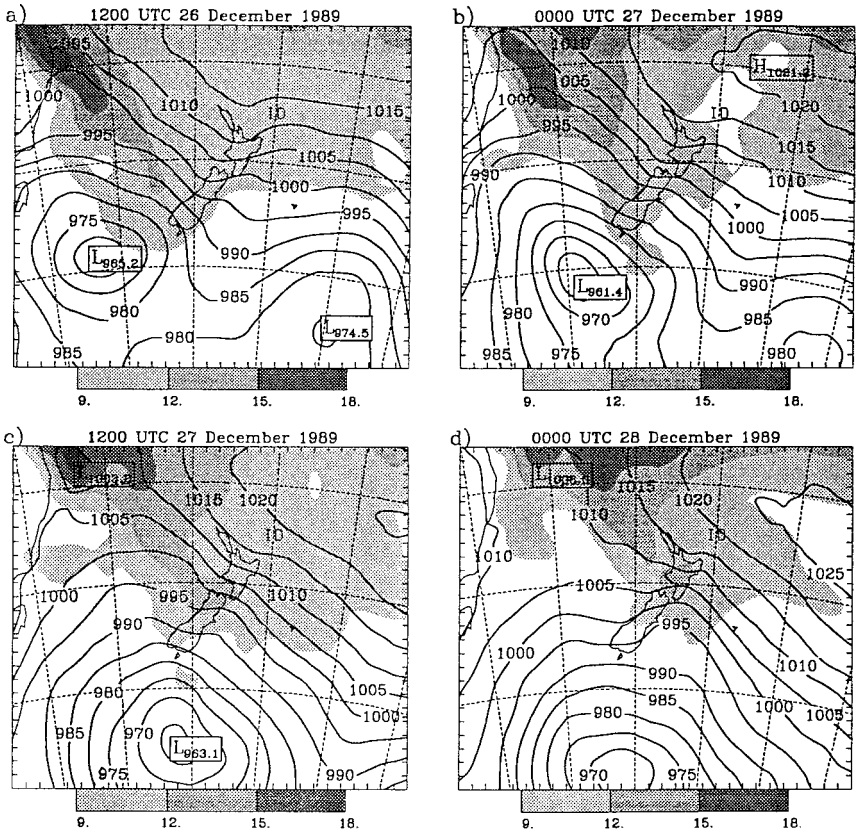

FIG. 25. ECWMF analysis of mean sea level pressure (solid, every 5 hPa) and 1000-hPa moisture (g kg^{-1}, shaded) at (a) 1200 UTC 26 Dec, (b) 0000 UTC 27 Dec, (c) 1200 UTC 27 Dec, and (d) 0000 UTC 28 Dec 1989 over New Zealand.

system.) Thus, for a quasi-stationary system, such as the convective system, which developed along the coast and subsequently along the windward (i.e., upslope) side of the Western Ghats, the critical level coincides with the wind reversal level. We hypothesize that this critical level tends to force the convective system to become stationary, which maximizes the vertical motion generated by the latent heating in the vicinity of the critical level (Lin 1987) and helps anchor the convective system to the upslope side of the Western Ghats, instead of being advected over to the plateau side, which produces long-lasting, persistent rainfall over both the coast and windward (i.e., upslope) regions (Fig. 28). In other words, the critical level plays the same role as the synoptic-scale high pressure ridge in the U.S. and Alpine cases, the typhoons in the Taiwanese cases, and the stationary front in the Japanese cases, all of which satisfy ingredient 8.

In Table 1, we have provided rough estimates for some of the common ingredients apparently responsible for producing heavy orographic rain in the United States, the European Alps, and east Asia. These include the low-level wind (U), mountain slope ($\partial h/\partial x$), water vapor mixing ratio (q), and CAPE. Note that w_{env} is difficult to estimate without fine-resolution data, so that we just denote whether or not there is an approaching synoptic-scale system (such as a deep short-wave trough), which is able to enhance the low-level, orographically forced upward vertical motion. It is also difficult to estimate the horizontal scale of the convective system and its propagation speed (c_s). On the other hand, even if we can estimate the propagation speed of the convective system accurately, the product on the right-hand side of Eq. (8) will be particularly sensitive to this value, especially when the convective system becomes stationary. Thus, as a first attempt, we only provide estimates for U, $\partial h/\partial x$, and q and propose $U(\partial h/\partial x)q$ as a new index. We then compare this index with the maximum observed rainfall rate. Although this proposed index is just a rough estimate, it appears that for the Taiwanese and Japanese cases, it has a relatively high value (e.g., >6) and the proposed index is roughly proportional to the observed maximum rainfall rates. The difference between the two Taiwanese cases is mainly due to the difference in the incoming flow speed (U). For U.S. events, it appears that the index has a lower value, but is still >2.7. With w_{env} included, the index should be able to reach a higher value (comparable to those estimated for the Taiwanese and Japanese cases). For Alpine events, the index is >4.7 (except for

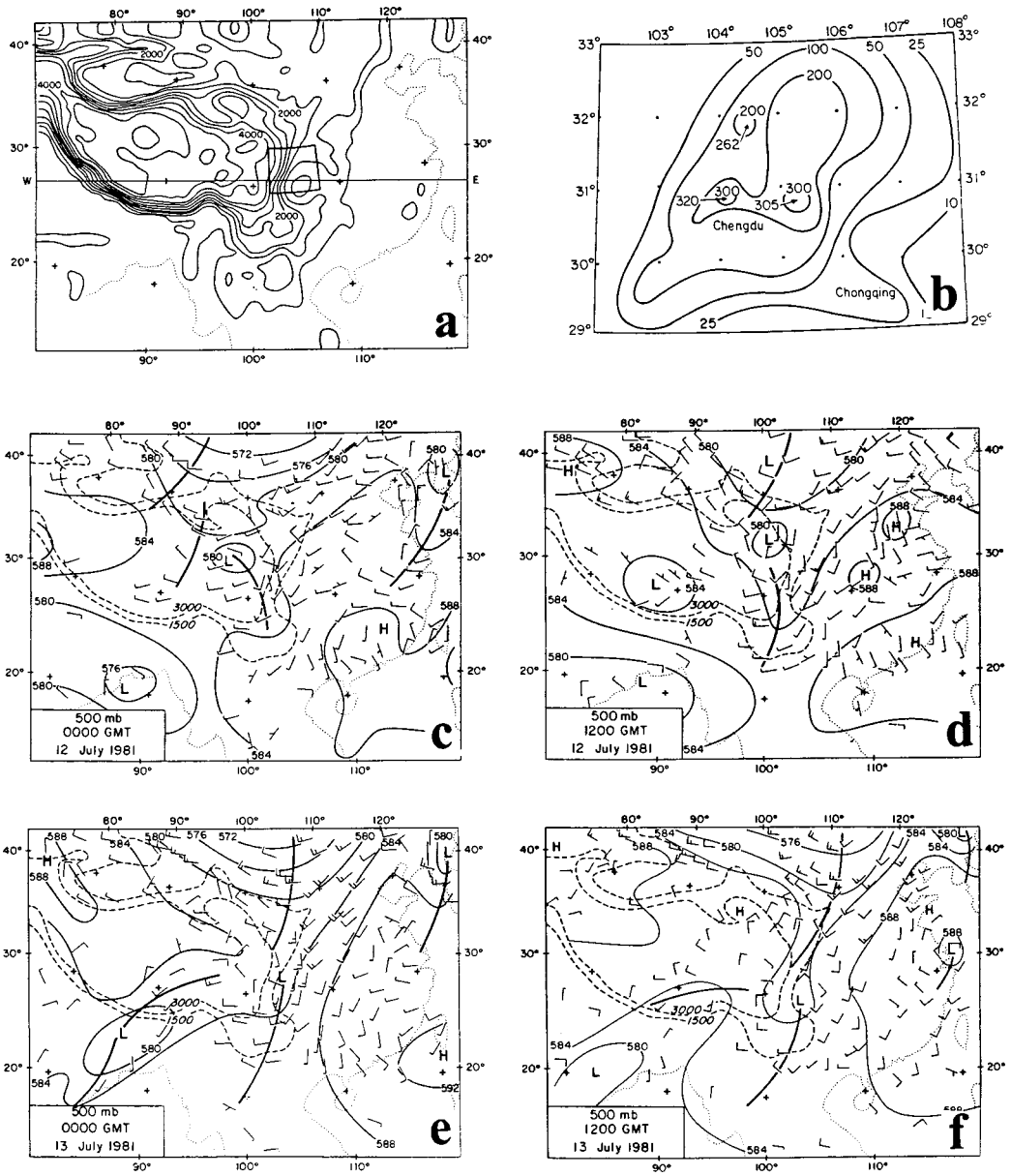

FIG. 26. (a) Topography of Sichuan basin, China, and the Tibetan Plateau. (b) The 48-h precipitation (in mm) ending at 0000 UTC 14 Jul over the Sichuan province. The 500-hPa analyses are shown at (c) 0000 UTC 12 Jul, (d) 1200 UTC 12 Jul, (e) 0000 UTC 13 Jul, and (f) 1200 UTC 13 Jul 1981. One full barb denotes 10 m s^{-1}. Solid contours are geopotential height (dam). [After Kuo et al. (1986).]

the South Ticino case). Therefore, this proposed index may help provide additionally valuable information for helping to predict the occurrence of upstream heavy orographic rainfall events. A more complete index may provide additional information in forecasting heavy orographic rainfall, especially with the help from finer-resolution numerical model data.

6. Concluding remarks

In this study, we have used common synoptic and mesoscale environmental features conducive to heavy orographic rainfall events found in the United States, and investigated whether similar situations exist in the European Alps, Taiwan, and Japan. Similar to U.S. events, the following common features are also observed in the European and east Asian cases: 1) a conditionally or potentially unstable airstream impinging on the mountains, 2) the presence of a very moist and moderate to intense LLJ, 3) the presence of steep orography to help release the conditional or convective instability, and 4) the presence of a quasi-stationary synoptic-scale system is required to impede or slow the progress of the orographically forced convective system

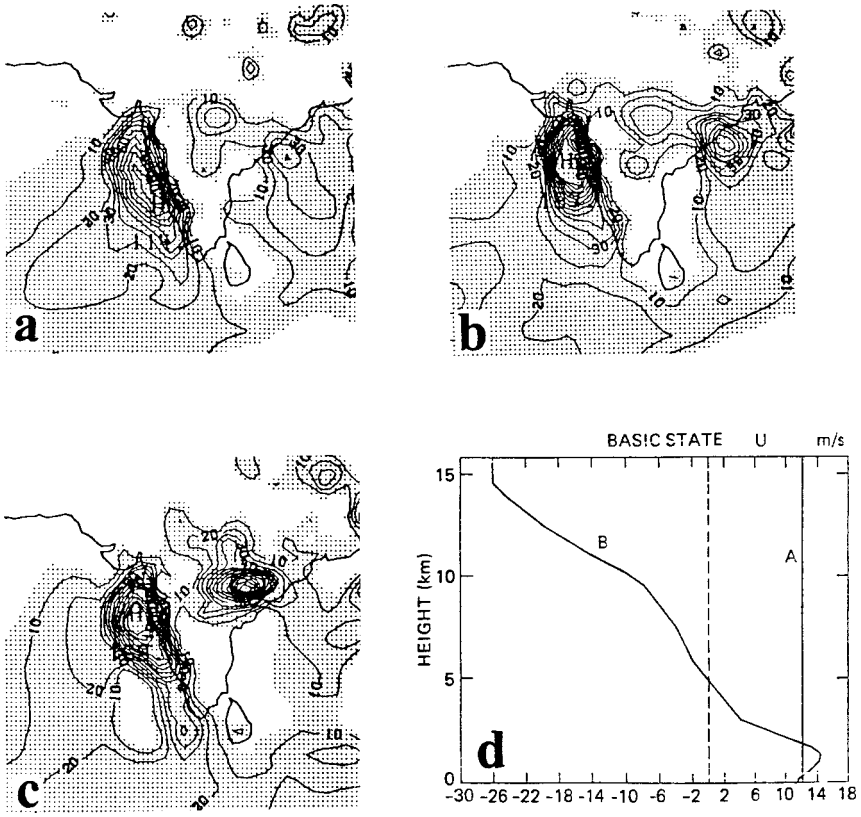

FIG. 27. Precipitation intensity (mm day^{-1}) estimated from satellite and rain gauge data over India and the Arabian Sea on (a) 23, (b) 24, and (c) 25 Jun 1979. The maximum values in rainfall intensity are 114, 197, and 169 mm day^{-1} on 23, 24, and 25 Jun, respectively. (d) The vertical profile of the east–west component of the wind. The shaded areas are mean precipitation areas. [After Ogura and Yoshizaki (1988).]

over the threat area. A deep short-wave trough or positive PV anomaly is found to approach the threat area in both the U.S. and Alpine cases, but is absent in the east Asian cases. On the other hand, high values of CAPE are observed in the east Asian cases, but are not consistently observed in either the U.S. or Alpine cases. In both the U.S. and Alpine cases, an approaching deep short-wave trough tends to 1) induce a low-level jet perpendicular to the mountain range, 2) reduce the static stability beneath the upper-level PV anomaly, and 3) enhance orographically induced upward motion on the trough's forward flank to trigger or enhance the convection. Thus, the last two processes may partially compensate the roles played by the high CAPE present in the east Asian cases. The quasi-stationary synoptic system can be 1) an upper-tropospheric high pressure ridge located to the west (east) of the threat area for heavy orographic rainfall events in the United States (European Alps), or 2) a typhoon (Taiwanese cases), or a front (Japanese case). In any event, these features act to retard or impede the convective system, which helps produce long-lasting, persistent rainfall. In both the Alpine and Taiwanese cases, convection often starts in a concave region of the mountain, which induces confluent flow and enhances the upward vertical motion. In the east Asian cases, we also find that *a significant amount of heavy rainfall may be triggered by orographic effects on the incoming conditionally or potentially unstable flow, instead of being directly associated with the convection already embedded within the tropical storm or depression.*

In order to better understand the dynamical basis for the common synoptic and mesoscale environmental features associated with heavy orographic rainfall in the mountains in the United States, the European Alps, Taiwan, and Japan, we extended the ''ingredient-based methodology'' for heavy orographic rainfall forecasting over a flat surface proposed by Doswell et al. (1996) to heavy orographic rainfall over mesoscale mountains. In taking this approach, we decomposed (partitioned) the low-level vertical velocity into synoptically forced (w_{env} and orographically forced (w_{oro}) components, and applied the lower boundary condition for flow over a mountain to obtain an algebraic expression for w_{oro}. In addition, a conditionally or potentially unstable airstream is needed to trigger deep convection. Based on this argument, we found that heavy orographic rainfall requires significant contributions from any combination

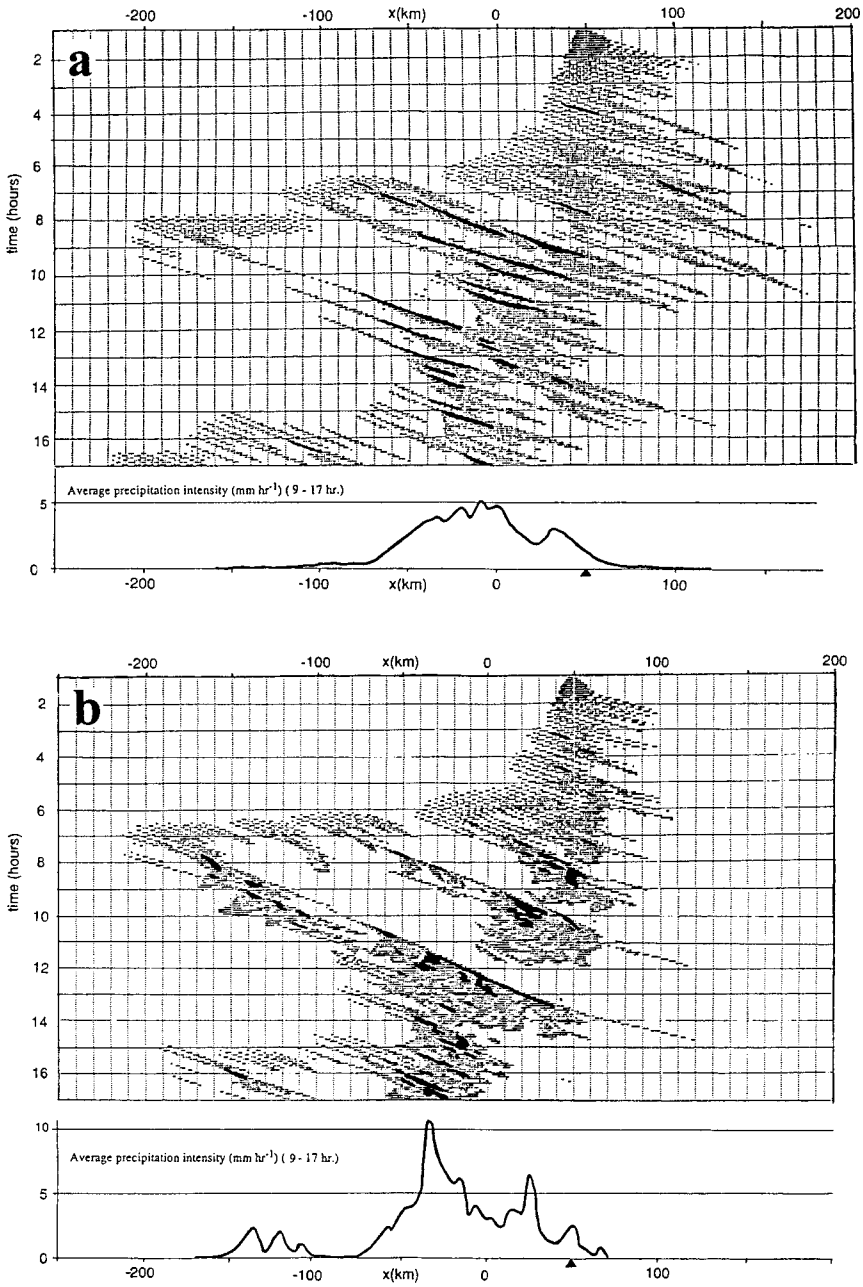

FIG. 28. (a) Temporal variation of precipitation intensity (mm h^{-1}) at the surface (upper panel) and the mean precipitation intensity averaged over 9–17 h (lower panel) in a case (case 3C of Ogura and Yoshizaki) with uniform basic flow; (b) same as in (a) except for a case with sheared basic flow with wind reversal level as shown in Fig. 27d (case 4C of Ogura and Yoshizaki). The location $x = 0$ represents the coastline and the solid triangle at $x = 50$ km denotes the position of the mountain peak. [After Ogura and Yoshizaki (1988).]

of the following common ingredients: 1) high precipitation efficiency of the incoming airstream; 2) the presence of a moist, moderate to intense LLJ; 3) steep orography to help release the instability; 4) favorable (e.g., concave) mountain geometry and a confluent flow field; 5) strong environmentally forced upward vertical motion; 6) the presence of a high moisture flow upstream; 7) a preexisting large-scale convective system; 8) slow (impeded or retarded) movement of the convective system; and 9) a conditionally or potentially unstable upstream airflow. The common synoptic and mesoscale environmental features conducive to heavy orographic rainfall events observed in the United States, Europe, and east Asia appear to belong to this set of common

ingredients. In addition, these common ingredients are also used to help explain the synoptic and mesoscale environments observed in some heavy orographic rainfall events, which have occurred in China, New Zealand, and India.

We also proposed an index, $U(\partial h/\partial x)q$, where U is the low-level flow velocity perpendicular to the mountain range, $\partial h/\partial x$ the mountain slope parallel to the basic flow, and q the low-level water vapor mixing ratio, to help predict the occurrence of heavy orographic rainfall. For the Taiwanese and Japanese cases, this index is >6 and the proposed index is roughly proportional to the observed maximum rainfall rates. For U.S. events, the index has a lower value, but is still >2.7. With w_{env} included, the index should be able to reach a value comparable to that for the Taiwanese and Japanese cases. For Alpine cases, the index is >4.7 (except for the South Ticino case). Therefore, this quantity may serve to provide additional information as an index for the prediction of the occurrence of heavy orographic rainfall. Due to the highly inherent temporal and spatial variation of the sounding data, estimates of this index may not be very accurate. However, it may be improved by using finer-resolution numerical model output and a more complete form, such as $(\mathbf{V}_H \cdot \nabla h)q$, which will help to better predict the distribution of heavy upslope rainfall. In addition, the proposed index and Eq. (8) do not include effects of conditional and potential instabilities; thus, the index may underestimate precipitation amounts.

In order to make a first attempt in the ingredient approach, we have decomposed (partitioned) the low-level upward vertical motion into environmentally forced and orographically forced components. It should be kept in mind that both the orographic and environmental forcing may interact nonlinearly to enhance the low-level upward vertical motion. For example, the LLJ may be enhanced by the approaching synoptic-scale system (such as a midtropospheric short-wave trough in U.S. and Alpine cases), which may increase the orographically forced upward vertical motion. However, if $\mathbf{V}_H$ is measured at a time and location close to the occurrence of the event, then the nonlinear contribution from the approaching synoptic-scale system to w_{oro} will be partially absorbed into $\mathbf{V}_H$.

Acknowledgments. We would like to thank Drs. C.-P. Pu and C.-W. Lee at the Civil Aeronautics and Aviation Administration of Taiwan for helping collect the data for this study, and also Dr. B.-W. Shen and Mr. G. Lai at the NASA Goddard Space Flight Center for setting up the numerical simulations in a parallel, but separate study. Dr. J. J. Charney, J. A. Thurman, and D. B. Engsley at NCSU helped in generating some of the figures. Discussions with Dr. C.-S. Chen at the National Central University of Taiwan and Dr. M. Yoshizaki at MRI of Japan are appreciated. Mr. H. Sakakibara at MRI of Japan has provided the soundings for the Japan case. Critical reviews of two anonymous reviewers are appreciated. This research is supported by National Sciences Foundation Grant ATM-0096876.

REFERENCES

Alpert, P. 1986: Mesoscale indexing of the distribution of orographic precipitation over high mountains. *J. Climate Appl. Meteor.*, **25,** 532–545.

Binder, P., and C. Schär, Eds., 1996: MAP design proposal. MeteoSwiss, 75 pp. [Available from MAP Programme Office, MeteoSwiss, CH-8044 Zurich, Switzerland.]

Bougeault, P., and Coauthors, 2001: The MAP special observing period. *Bull. Amer. Meteor. Soc.*, **82,** 433–462.

Buzzi, A., and L. Foschini, 2000: Mesoscale meteorological features associated with heavy precipitation in the southern Alpine region. *Meteor. Atmos. Phys.*, **72,** 131–146.

——, N. Tartaglione, C. Cacciamano, T. Paccagnella, and P. Patruno, 1995: Preliminary meteorological analysis of the Piedmont flood of November 1994. *MAP Newsletter*, No. 2, 2–6.

——, ——, and P. Malguzzi, 1998: Numerical simulations of the 1994 Piemont flood: Role of orography and moist processes. *Mon. Wea. Rev.*, **126,** 2369–2383.

Caracena, F., and J. M. Fritsch, 1983: Focusing mechanisms in the Texas Hill Country flash floods of 1978. *Mon. Wea. Rev.*, **111,** 2319–2332.

——, R. A. Maddox, L. R. Hoxit, and C. F. Chappell, 1979: Mesoanalysis of the Big Thompson storm. *Mon. Wea. Rev.*, **107,** 1–17.

Chen, G. T.-J., and C.-C. Yu, 1988: Study of low-level jet and extreme heavy rainfall for northern Taiwan in the mei-yu season. *Mon. Wea. Rev.*, **116,** 884–891.

Chen, S.-H., and Y.-L. Lin, 2001: Regimes for conditionally unstable flow over an idealized three-dimensional mesoscale mountain. Preprint, *Ninth Conf. on Mesoscale Processes*, Fort Lauderdale, FL, Amer. Meteor. Soc., 405–408.

Chu, C.-M., and Y.-L. Lin, 2000: Effects of orography on the generation and propagation of mesoscale convective systems in a two-dimensional conditionally unstable flow. *J. Atmos. Sci.*, **57,** 3817–3837.

Doswell, C. A., III, H. Brooks, and R. Maddox, 1996: Flash flood forecasting: An ingredient-based methodology. *Wea. Forecasting*, **11,** 560–581.

——, R. Romero, and S. Alonso, 1998: A diagnostic study of three heavy precipitation episodes in the western Mediterranean region. *Wea. Forecasting*, **13,** 102–124.

Fehlmann, R., and C. Quadri, 2000: Predictability issues of heavy Alpine south-side precipitation. *Meteor. Atmos. Phys.*, **72,** 223–231.

Houze, R. A., 1993: *Cloud Dynamics*. Academic Press, 573 pp.

——, and S. Medina, 2000: Two cases of heavy rain on the Mediterranean side of the Alps in MAP. Preprints, *Ninth Conf. on Mountain Meteorology*, Aspen, CO, Amer. Meteor. Soc., 1–5.

Katzfey, J. J., 1995: Simulation of extreme New Zealand precipitation events. Part II: Mechanisms of precipitation development. *Mon. Wea. Rev.*, **123,** 755–775.

Kelly, W. E., and D. R. Mock, 1982: A diagnostic study of upper tropospheric cold lows over the western North Pacific. *Mon. Wea. Rev.*, **110,** 471–480.

Kuo, Y.-H., L. Cheng, and R. A. Anthes, 1986: Mesoscale analysis of the Sichuan flood catastrophe, 11–15 July 1981. *Mon. Wea. Rev.*, **114,** 1984–2003.

Lin, Y.-L., 1987: Two-dimensional response of a stably stratified shear flow to diabatic heating. *J. Atmos. Sci.*, **44,** 1375–1393.

——, 1993: Orographic effects on airflow and mesoscale weather systems over Taiwan. *Terr. Ocean. Atmos.*, **4,** 381–420.

Maddox, R. A., L. R. Hoxit, C. F. Chappell, and F. Caracena, 1978: Comparison of meteorological aspects of the Big Thompson and Rapid City flash floods. *Mon. Wea. Rev.*, **106,** 375–389.

——, F. Canova, and L. R. Hoxit, 1980: Meteorological character-

istics of flash flood events over the western United States. *Mon. Wea. Rev.*, **108,** 1866–1877.

Massacand, A. C., H. Wernli, and H. C. Davies, 1998: Heavy precipitation on the Alpine southside: An upper-level precursor. *Geophys. Res. Lett.*, **25,** 1435–1438.

Ogura, Y., and M. Yoshizaki, 1988: Numerical study of orographic–convective precipitation over the eastern Arabian Sea and the Ghats Mountains during the summer monsoon. *J. Atmos. Sci.*, **45,** 2097–2122.

Petersen, W. A., and Coauthors, 1999: Mesoscale and radar observations of the Fort Collins flash flood of 28 July 1997. *Bull. Amer. Meteor. Soc.*, **80,** 191–216.

Pontrelli, M. D., G. Bryan, and J. M. Fritsch, 1999: The Madison County, Virginia, flash flood of 27 June 1995. *Wea. Forecasting,* **14,** 384–404.

Sakakibara, H., 1979: Cumulus development on the windward side of a mountain range in convectively unstable air mass. *J. Meteor. Soc. Japan*, **57,** 341–348.

Saucier, W. J., 1955: *Principles of Meteorological Analysis.* The University of Chicago Press, 438 pp.

Smith, R. B., 1979: The influence of mountains on the atmosphere. *Advances in Geophysics*, Vol. 21, Academic Press, 87–230.

——, and Y.-L. Lin, 1983: Orographic rain on the western Ghats. *Mountain Meteorology*, E. R. Reiter Z. Baozhen, and Q. Yongfu, Eds., Science Press and Amer. Meteor. Soc., 71–94.

——, and Coauthors, 1997: Local and remote effects of mountains on weather: Research needs and opportunities. *Bull. Amer. Meteor. Soc.*, **78,** 877–892.

Xue, M., K. K. Droegemeier, and V. Wong, 2000: The Advanced Regional Prediction System (ARPS)—A multi-scale nonhydrostatic atmospheric simulation and prediction model. Part I: Model dynamics and verification. *Meteor. Atmos. Phys.*, **75,** 161–193.